A Comparative Review of Wet and Dry Electrode Manufacturing Processes: Opportunities, Limitations, and Challenges in the Production of Lithium-Ion Battery Electrodes

REVIEW OPEN ACCESS

A Comparative Review of Wet and Dry Electrode Manufacturing Processes: Opportunities, Limitations, and Challenges in the Production of Lithium-Ion Battery Electrodes

Shoayb Mojtahedi[1,2,3] | Francesca Soavi[1,2]

[1]Department of Chemistry "Giacomo Ciamician", Alma Mater Studiorum University of Bologna, Bologna, Italy | [2]ENERCube Lab, Centro Ricerche Energia, Ambiente e Mare, Centro Interdipartimentale per la Ricerca Industriale Fonti, Rinnovabili, Ambiente, Mare ed Energia (CIRI-FRAME), Alma Mater Studiorum University of Bologna, Marina di Ravenna, Italy | [3]Department of Applied Science and Technology (DISAT), Polytechnic University of Turin, Turin, Italy

Correspondence: Shoayb Mojtahedi (Shoayb.mojtahedi@unibo.it) | Francesca Soavi (Francesca.soavi@unibo.it)

Received: 22 November 2025 | **Revised:** 23 January 2026 | **Accepted:** 25 January 2026

Keywords: dry processing | electrode fabrication | lithium-ion batteries | sustainability | wet processing

ABSTRACT

The rising demand for lithium-ion batteries (LIBs) highlights the importance of developing electrode fabrication methods that ensure high performance, cost efficiency, and environmental sustainability. Here, wet (slurry-based) and dry (solvent-free) electrode fabrication methods are compared with a focus on both anodes and cathodes. Despite its integration within an established industrial system, the wet method exhibits significant limitations stemming from the use of volatile solvents such as N-methyl-2-pyrrolidone (NMP), the high energy demand of the drying stage, and the complexity of scaling up thick electrode manufacturing. On the other hand, dry electrode fabrication eliminates the need for solvents, reduces energy use, simplifies production workflows, and improves mechanical integrity. The latter helps in the development of high-loading electrodes for next-generation high-energy density storage systems. However, dry processing introduces new technical challenges that must first be addressed, including binder activation, uniform material dispersion, the need for specialized hardware, and the development of customized equipment. By focusing on the underlying mechanisms, advantages, and practical limitations, this review aims to support the development of optimized electrode fabrication strategies that facilitate the widespread adoption of sustainable battery technologies.

1 | Introduction

Lithium-ion batteries (LIBs) have emerged as a key enabling technology for modern energy storage systems due to their superior energy density and cycling stability [1]. Since their commercial introduction in the early 1990s, LIBs have rapidly become the dominant technology for portable electronics [2]. Their applications have expanded into the electric vehicle and stationary storage markets, playing a crucial role in the integration of renewable energy sources [3]. In other words, LIBs have revolutionized energy storage, powering a wide range of applications from portable electronics to electric vehicles and renewable energy systems [4]. The design of LIB systems can be optimized for specific applications by carefully selecting the cell technology, system architecture, and operational strategy [5]. The choice of cell technology is rooted in the selection of electrode materials, which define the performance and safety characteristics of LIB systems. These material-level decisions influence the system architecture and dictate the requirements for thermal management and control. In turn, the operational strategy must be

tailored to the electrochemical behavior of the electrodes to minimize degradation and ensure long-term stability. As the demand for flexible energy systems grows, LIBs continue to evolve, addressing challenges related to production, distribution, and disposal [3].

LIBs consist of several key components that work together to enable efficient energy storage and release. These include the cathode, anode, electrolyte, separator, and current collectors [6]. Among these, the cathode and anode electrodes play a pivotal role in determining the battery's overall performance [7]. The cathode typically consists of lithiated inorganic compounds (e.g., lithium iron phosphate, $LiFePO_4$, lithium nickel manganese cobalt oxide, $LiNi_xMn_yCo_zO_2$), while the anode is commonly made of graphite or emerging high-capacity materials like silicon or lithium metal. These electrodes govern the battery's energy density, power output, and cycle life.

The manufacturing of electrodes involves coating active materials (AM) onto metallic current collectors (aluminum for the cathode and copper for the anode), which enable electron transfer during charging and discharging. The structure, composition, and quality of the electrodes significantly influence the battery's capacity, internal resistance, and cycle life [8–10]. As a result, the optimization of electrode materials and manufacturing processes is critical to enhancing LIB performance [11], reducing costs [12], and addressing environmental concerns associated with their production [13].

Traditional electrode manufacturing is a wet-coating process and is the backbone of LIB production. This conventional process is used to fabricate electrodes (both cathodes and anodes) by distributing slurries of AM, carbon conductive additive (CA), and binder onto the conductive current collector foil. On a lab scale, coating is performed using simple tools like the doctor blade, while industrial production relies on advanced slot-die coaters for precision and scalability. After drying, the coated electrodes are then compressed to achieve optimal density and performance [14]. The conventional electrode is formed through defined steps, such as slurry preparation, slurry coating, electrode drying, and calendering [15].

Conventional slurry casting processes offer several advantages but also come with notable limitations [9]. It allows for high material utilization and flexibility in formulation, accommodating various AMs, binders, and CAs. This process also ensures uniform material distribution across the electrode surface, leading to stable and reproducible electrochemical performance. These processes are well-established, scalable, and compatible with mass production using roll-to-roll manufacturing techniques [16]. However, the LIB industry faces environmental challenges due to its reliance on toxic solvents and energy-intensive drying processes. Conventional electrode manufacturing uses N-methyl-2-pyrrolidone (NMP), which is expensive, toxic, and energy-intensive to both produce and recycle during the drying process [17–19]. In addition, drying is one of the most energy-intensive processes in cell manufacturing and a significant contributor to greenhouse gas emissions [20]. To address these limitations of conventional manufacturing methods for LIBs, NMP-free and dry electrode manufacturing techniques, which offer potential benefits such as reduced energy consumption, lower costs, and improved environmental sustainability, are under development and exploitation [21–27].

A promising approach to addressing the limitations of conventional electrode manufacturing is dry electrode processing. This advanced technique eliminates the use of solvents such as NMP, thereby significantly reducing environmental impact, production complexity, and energy requirements. By removing the need for solvent recovery and drying steps, dry electrode processing offers a cleaner, more efficient, and cost-effective pathway for LIB production, making it a key innovation for sustainable energy storage solutions [28]. Moreover, dry electrode manufacturing enables easier fabrication of high-energy density storage systems by supporting the use of thick electrodes with improved mechanical integrity and uniformity [29]. The key features of wet (conventional) and dry electrode manufacturing methods are summarized in Table 1 [25, 30–32].

Several high-quality review articles have addressed either conventional slurry-based electrode manufacturing or emerging dry electrode technologies [33–36]. However, fewer studies have explicitly analyzed these two manufacturing paradigms side-by-side at the level of individual processing steps. As a result, the practical trade-offs between wet and dry manufacturing, particularly from an industrial and process-engineering perspective, remain insufficiently discussed [37, 38].

The objective of this review is therefore to offer a structured, process-level comparison between conventional wet and emerging dry electrode manufacturing methods. For each key manufacturing step from material preparation and processability to coating or film formation, drying, and calendaring, we directly compare the underlying mechanisms, advantages, limitations, and scalability challenges of both approaches. By adopting this comparative framework, this review aims to clarify how wet and dry processing differ in terms of physical mechanisms and process control. We highlight where dry manufacturing offers genuine advantages and where critical challenges remain and provide practical insights relevant to industrial scale-up and next-generation battery manufacturing.

Such a perspective is intended to complement existing reviews and to support informed decision-making for researchers and manufacturers seeking sustainable, high-performance electrode fabrication strategies.

To help the reader, Scheme 1 reports how this review is developed.

2 | Electrode Material Processing in Conventional Wet and Dry Electrode Manufacturing

As shown in Figure 1, conventional electrode fabrication involves sequential steps, including slurry preparation, coating, drying, and calendering and each of these steps are important to achieve a high-quality electrode.

Dry electrode manufacturing is an emerging, solvent-free process for producing LIB electrodes. Unlike traditional slurry-based methods, it eliminates the use of liquid solvents and drying steps, offering potential advantages in cost, energy consumption, and environmental impact. Figure 2 illustrates the dry electrode manufacturing steps, together with the corresponding equipment and changes in electrode material properties throughout the process [39].

TABLE 1 | Key features of wet and dry electrode manufacturing.

	Wet electrode manufacturing	Dry electrode manufacturing
Scalability	Well-established, widely used in commercial settings.	Emerging technology with strong potential for high-volume scalability.
Material uniformity	Excellent, aided by solvent-based slurry formation.	Enhanced control over porosity and thickness due to solid-state processing.
Environmental impact	Utilizing recyclable solvents like NMP but still involving volatile organic compounds (VOCs).	Solvent-free process, eliminating VOCs.
Energy efficiency	Moderate due to energy required for drying and solvent recovery.	High, due to eliminating drying and solvent recovery steps.
Cost CAPEX, Capital expenditure	CAPEX, Relatively high, up to 20% greater, primarily due to the need for solvent recovery units and drying infrastructure.	CAPEX, Reduced by approximately 10%–15% owing to the elimination of solvent handling and drying stages, resulting in a more streamlined production line.
OPEX, Operating expenditure	OPEX, Significant ongoing cost, as NMP solvent accounts for approximately 11.5% of total manufacturing costs and more than 46% of total energy consumption.	OPEX, Lower by an estimated 10%–20% due to decreased energy demand and the absence of solvent-related costs.
Process Safety & Handling	Uses solvents (e.g., NMP) that require careful handling and disposal.	Solvent-free process requires complex equipment.
Energy usage	Energy-intensive drying and solvent recovery steps.	Equipment for dry processing is still developing.
Adoption	Industry standard with established supply chains.	Limited adoption due to nascent technology.
Binder adhesion	Slurry binders provide good adhesion.	Ensuring consistent adhesion without liquid binders is a challenge.
Battery types	Suitable for most commercial lithium-ion batteries.	Suitable for next-gen and high-energy-density batteries.
Electrode thickness	Well-suited for thin electrode fabrication.	Ideal for thicker electrodes in energy-dense cells.

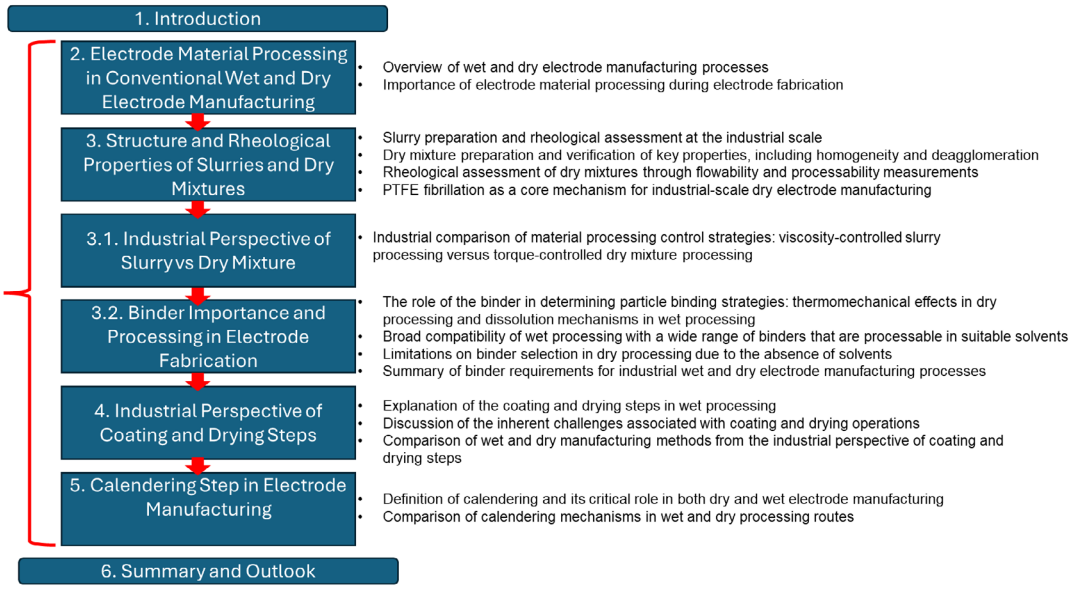

SCHEME 1 | Structure of the present review and summary of each section.

The dry electrode manufacturing process generally consists of two principal steps, as illustrated in Figure 3, namely, dry powder mixing and subsequent lamination/calendering of either the dry-mixed powder blend or a free-standing film onto the current collector. In the dry mixing step, AMs, binder (often PTFE or similar fibrillating binders), and CAs are dry-blended to form a homogenous powder mixture. In the film formation process, the mixture is processed to form a cohesive dry film by using

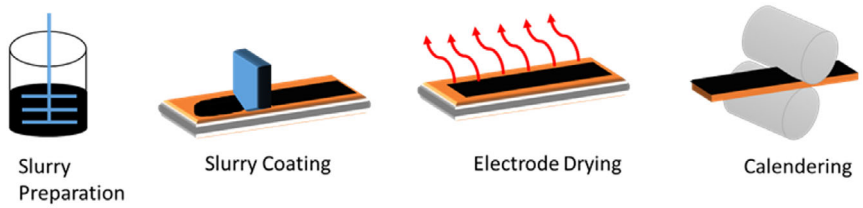

FIGURE 1 | Wet electrode manufacturing steps.

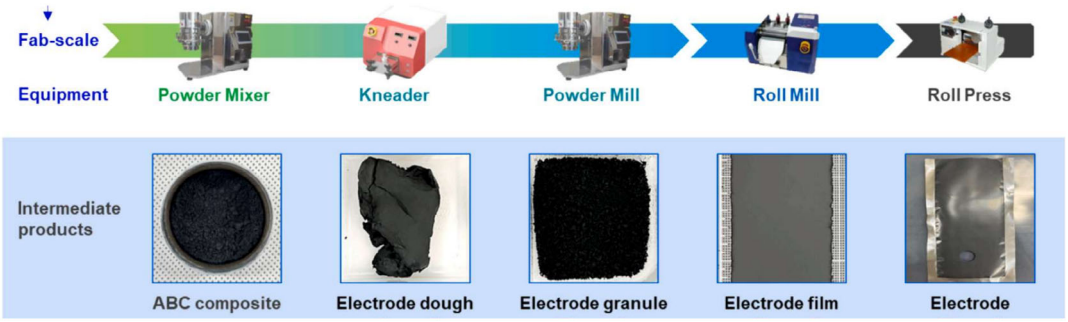

FIGURE 2 | Dry electrode manufacturing steps and equipment for fabricating a LIB cathode electrode composed of polytetrafluoroethylene (PTFE) binder, single-crystal $LiNi_{0.8}Co_{0.1}Mn_{0.1}O_2$ (NCM811) active material, and carbon black (CB, Super P) and carbon nanotube (CNT) conductive agents [39]. Reproduced (Adapted) with permission, Copyright 2024, Elsevier.

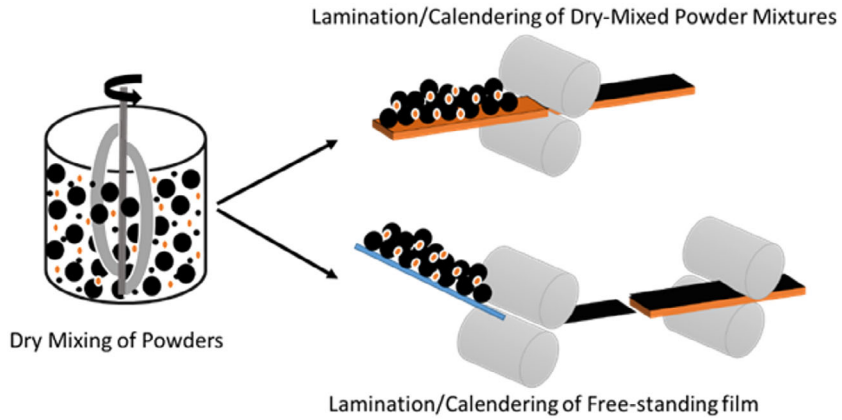

FIGURE 3 | Schematic of the dry electrode manufacturing process.

extrusion, roll pressing, or other mechanical compaction methods. Finally, during the lamination or calendering, either the dry-mixed powder blend or the free-standing film is laminated or calendared directly onto the current collector (copper for anodes, aluminum for cathodes) under pressure and sometimes heat to ensure adhesion and mechanical integrity.

Material processing represents the first decisive step in LIB electrode manufacturing, as it determines the homogeneity, process stability, and scalability of all downstream operations. At the industrial level, inadequate control at this stage propagates defects throughout the manufacturing line, leading to yield losses, inconsistent electrode quality, and increased production costs. While both wet and dry manufacturing aim to achieve uniform distribution of AMs, CAs, and binders, they rely on fundamentally different physical principles and process controls. To clearly highlight these differences, wet and dry material processing routes are discussed side-by-side below, with explicit emphasis on industrial process requirements.

3 | Structure and Rheological Properties of Slurries and Dry Mixtures

The wet manufacturing route begins with the preparation of a homogeneous mixture, commonly known as a slurry, which includes several key components: AM (e.g., lithium metal oxides for cathodes or graphite for anodes), serving as the primary energy-storing component; CA (e.g., carbon black (CB)), which enhances electrical conductivity, binders (e.g., polymers like polyvinylidene fluoride (PVDF)), which hold the AM and CA together, and a solvent (e.g., NMP), used to dissolve the binder and facilitate mixing. These materials are combined using high-shear mixers to ensure uniform distribution of particles, resulting in a consistent and well-mixed slurry ready for the subsequent coating process [16].

Rheology is the study of the flow and deformation of materials. It provides valuable insights into the slurry's structure, stability, and processability [40]. The rheological properties of LIB electrode slurries play a pivotal role in determining their processing behavior, coating quality, and the overall performance of the

resulting electrodes [41]. Understanding the interactions among slurry components, including AM, CA, binder, and solvent, is essential for optimizing electrode manufacturing processes, enhancing performance, and ensuring sustainability [41].

Viscosity is a fundamental property of fluids that measures their resistance to flow. It describes the internal friction within a fluid, which is influenced by the interactions between its molecules [42]. The relationship between viscosity, shear stress (SS), and shear rate provides critical insights into the behavior of fluids under stress and is particularly relevant in fields such as rheology, fluid dynamics, and materials science [43, 44].

SS is the force per unit area applied parallel to a surface within a material, causing deformation. It describes how much stress is exerted by the fluid layers sliding past one another. In fluids, SS arises when there is relative motion between adjacent layers of fluid, such as during flow in a pipe or while stirring. Mathematically, SS is expressed as [45]:

$$\tau = \frac{F}{A} \tag{1}$$

where τ, F, and A represent the SS (N/m^2), the force (N), and the area over which the force is distributed (m^2), respectively. Shear rate represents the rate at which the deformation occurs within the fluid. It measures how quickly one layer of fluid moves relative to another. The shear rate is defined as the velocity gradient perpendicular to the direction of flow [46]:

$$\dot{\gamma} = \frac{dv}{dy} \tag{2}$$

where the $\dot{\gamma}$, v, and y denote the shear rate (1/s), the fluid velocity in the flow direction (m/s) and the distance perpendicular to the flow direction (m), respectively. Viscosity links the applied SS and the resulting shear rate in a fluid. Then, the viscosity is expressed as the ratio of SS to shear rate:

$$\eta = \frac{\tau}{\dot{\gamma}} \tag{3}$$

For Newtonian fluids (e.g., water, air, and most simple liquids), viscosity remains constant regardless of the shear rate. Their behavior is linear, meaning that SS is directly proportional to shear rate. Non-Newtonian fluids, on the other hand, exhibit viscosity that changes with shear rate. This behavior is classified into two types: shear-thinning and shear-thickening fluids. The viscosity of shear-thinning fluids decreases as the shear rate increases. Conversely, the viscosity of shear-thickening fluids increases as the shear rate rises [43, 47, 48].

Electrode slurries typically exhibit shear-thinning properties [49]. At low shear rates (e.g., when at rest), the viscosity is high, preventing particle settling. At high-shear rates (e.g., during mixing or coating), the viscosity decreases, facilitating easier spreading and application. The slurry must achieve a specific SS to flow efficiently [50]. The appropriate balance ensures thorough mixing without damaging sensitive materials [51]. Therefore, the appropriate shear rates during mixing break up agglomerates of AMs and conductive agents, ensuring a homogeneous mixture. Viscosity must be controlled to facilitate particle dispersion without excessive heat generation. Slurry must flow through pipelines or equipment with minimal resistance [40]. Moreover, achieving the appropriate viscosity range and optimal component ratio is essential for forming a proper coating on the current collector [52]. Consistent viscosity at operating shear rates ensures smooth transport. During electrode coating (e.g., using a slot-die coater), the shear rate increases as the slurry is forced through narrow gaps. The slurry's shear-thinning property ensures that a uniform thin film is applied smoothly. At the same time, a high enough viscosity on the substrate is required to prevent unwanted fluid movement, such as flowing downward (running) or pooling in certain areas (spreading unevenly). Furthermore, proper viscosity control prevents cracking or uneven surfaces during drying, directly impacting battery performance and longevity.

To achieve the desired rheological properties, manufacturers carefully adjust several factors. Solvent content controls the base viscosity of the slurry, while binder concentration affects its elasticity and flow behavior. Particle size distribution influences shear rate dependency and overall flow characteristics, and mixing time and speed determine the homogeneity of the mixture. Each of these parameters plays a crucial role in optimizing the slurry's performance during the preparation and coating processes [49].

Several models can accurately fit experimental slurry data, including the traditional Cross model [53], the Bingham model, and the Cross model with yield stress [54]. The choice of model depends on the solid content and formulation of the slurry. Figure 4 illustrates how viscosity varies with shear rate for different solid content levels in a slurry.

For high-solid-content slurries, a minimum SS limit is required for the flow and proper spreading on the current collector. The applied SS must exceed the slurry's yield stress, which is defined as the critical stress required to initiate irreversible deformation and flow. The yield stress thus represents the transition point between elastic (solid-like) and viscous (liquid-like) behavior. Below this threshold, the slurry deforms elastically under applied stress, whereas above it, the material yields and begins to flow continuously [55]. The Bingham model is commonly used to fit high-solid content slurry data, as it accounts for this yield stress.

In contrast, the Cross model is suitable for low-solid-content slurries, where flow begins at any applied SS. For medium solid content slurries, the Cross model provides a more accurate fit, as it captures both shear-thinning behavior and the presence of a yield SS.

C. D. Reynolds et al. examined the rheological properties of two industrially relevant battery electrode slurries (anode and cathode), finding that specific material compositions and solid

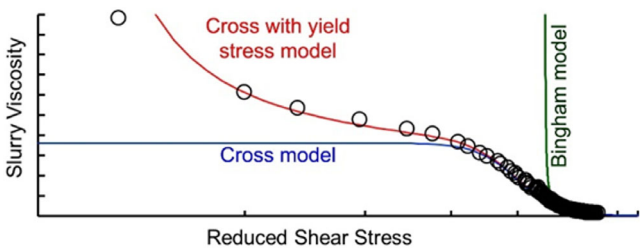

FIGURE 4 | Variation of viscosity with shear rate for different solid content levels in a slurry [54]. Reproduced (Adapted) with permission, Copyright 2019, Elsevier.

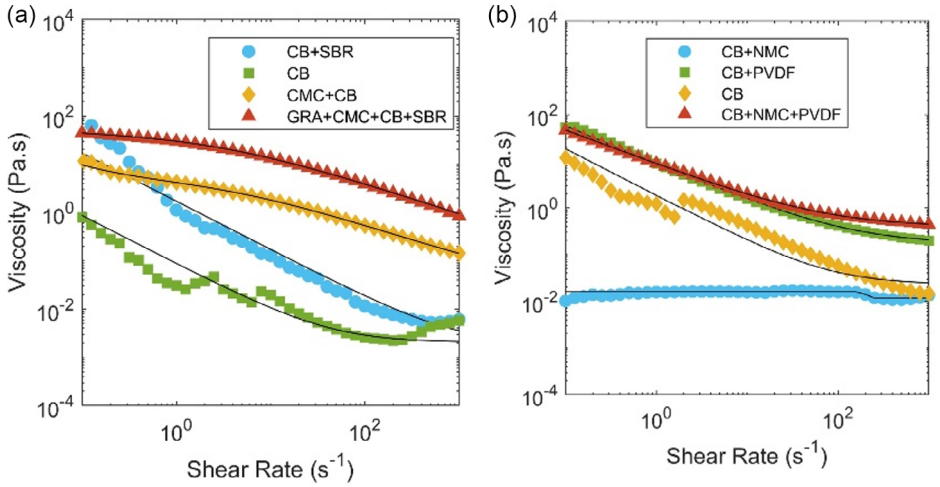

FIGURE 5 | Flow curves of all components of an industrial (a) anode (graphite (GRA), carbon black (CB), carboxymethyl cellulose (CMC), and styrene–butadiene rubber (SBR) in water) and (b) cathode (NMC, CB, and PVDF in NMP) slurries, black lines indicate fits with the Cross model with a yield stress [41]. Reproduced (Adapted) from Reynolds et al. [41] (CC BY 4.0). Copyright 2020, Wiley.

concentrations significantly impact viscosity and flow characteristics. Both slurries exhibited shear-thinning behavior, and their rheological data were accurately modeled using the Cross model with yield stress [41]. As shown in Figure 5, the flow curves of both anode and cathode slurries, as well as those of their individual component combinations (anode: graphite (GRA), CB, carboxymethyl cellulose (CMC), and styrene–butadiene rubber (SBR) in water; cathode: $LiNi_xMn_yCo_zO_2$ (NMC), CB, and PVDF in NMP) indicate that the Cross model with yield stress provides an accurate fit to the experimental rheological data.

Each coating line provides a particular yield stress for spreading the slurry onto the current collector. This yield stress must be compatible with the slurry rheology data. Hence, analyzing the variation of slurry viscosity at different shear rates provides insight into whether the slurry is ready for introduction into the coating line. In other words, the yield stress is a crucial rheological parameter that dictates how easily an electrode slurry will spread during the coating process. It represents the minimum amount of force (stress) required for the slurry to begin flowing like a liquid. For a battery manufacturing line to operate efficiently, the specific yield stress provided by the coating equipment must be compatible with the inherent rheology of the slurry mixture. If the slurry's yield stress is too high, it may not spread uniformly under the shear forces of the coater, potentially leading to defects, inconsistent electrode thickness, and uneven AM distribution [41, 56, 57]. Therefore, optimizing the slurry formulation to achieve a compatible yield stress is essential for robust and high-quality battery production.

During mixing, the slurry components experience mechanical torque from the mixer blades, significantly influencing the slurry's rheology. Therefore, measuring the mixer torque is essential for determining SS and shear rate, enabling an operando system where slurry rheology is monitored in real time during mixing. Recognizing the significance of determining rheological properties through torque, G. Ronnie et al. developed a combined rheometer/mixer to analyze the rheological characteristics of fluids [58]. As shown in Figure 6, the rheometer/mixer evaluates torque (T) generated by the relative rotation between the stator and rotor at varying rotational speeds (RPMs).

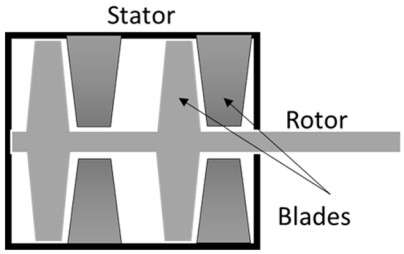

FIGURE 6 | The rheometer/mixer including a stator and rotor having some blades.

SS and volume-averaged shear rate (VASR) are determined using the following equations:

$$\begin{cases} SS = T^{\beta}/K \\ VASR = K_1(RPM)^{\alpha} \end{cases} \quad (4)$$

where K, k_1, α, and β are experimentally-derived coefficients [58]. In this way, the rheometer/mixer can simultaneously blend the electrode components in the solvent and measure the resulting slurry rheology, enabling straightforward optimization of slurry properties.

Slurry agglomerates are clusters of AM particles, CA, and binder that form due to interparticle forces. The size and shape of these agglomerates play a critical role in defining the rheological properties, coating uniformity, and overall electrode performance of LIB slurries [41]. When agglomerates approach the coating gap size, they can cause frictional effects, leading to increased pressure, coating defects, or even making the coating process unfeasible. Therefore, aggregates of a similar size to the coating gap are undesirable. The agglomerate size distribution impacts slurry stability, viscosity, and dispersion efficiency. Thus, controlling agglomeration is crucial for ensuring a stable and high-performance electrode slurry [16]. The Hegman gauge is a manual tool used to roughly quantify aggregates that are comparable in size to the coating gap [59]. Figure 7 illustrates the influence of slurry aggregation and particle-size distribution on coating quality [60]. As shown, a nonuniform slurry containing pronounced

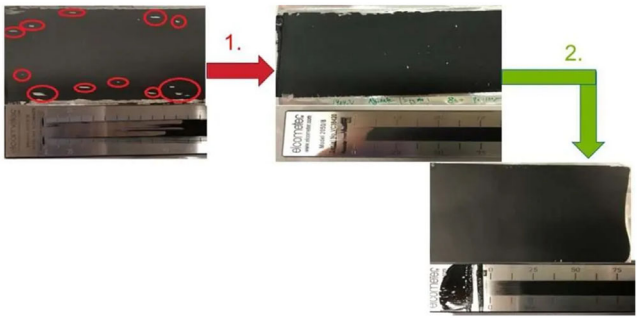

FIGURE 7 | Hegman gauge (grindometer) analysis demonstrating the transition from aggregated slurry to homogeneous dispersion [60]. Reproduced (Adapted) with permission from Giar Alsofi et al.

agglomerates leads to visible defects in the resulting electrode coating. In contrast, formulation optimization promotes a homogeneous dispersion with minimal residual aggregates, thereby enabling a uniform, defect-free coating and improved electrode quality.

In addition to flow-related parameters such as viscosity and agglomerate morphology, the interfacial and surface properties of the slurry are equally critical, as they govern slurry stability and can induce nonuniformities during the coating process [61]. The contact angle of the slurry on the current collector is a micromechanical property influenced by the surface tension between the slurry and air, the interfacial tension between the slurry and the current collector, and the free energy of the collector surface. These factors are primarily determined by the slurry formulation and mixing process. A high contact angle can lead to poor wetting, resulting in holes and defects in the coating. Conversely, a low contact angle causes excessive spreading of the slurry, making it challenging to achieve a well-defined and uniform coating. Additionally, water-based slurries generally exhibit higher surface tension compared to NMP-based slurries, which can introduce issues such as electrode cracking during drying [62]. Proper formulation adjustments are necessary to optimize wettability and coating performance [63].

The dry mixing of powders is the initial step in dry electrode manufacturing, typically carried out using a dry high-shear mixer, planetary mixer, or Bead mill homogenizer [26, 64, 65]. Figure 8 presents schematic representations of the mixers commonly employed for powder processing. In a planetary mixer (Figure 8a), the mixing tool undergoes simultaneous rotation and revolution, analogous to a planet orbiting the sun. This combined motion continuously drives powders toward the mixing element, facilitating efficient dispersion and the formation of a uniform mixture. In a bead mill (Figure 8b), energy is imparted to the grinding beads through an agitator mounted on a rotating spindle, the resulting bead–particle interactions effectively break down agglomerates and yield a homogeneous powder blend. By contrast, a high-shear mixer (Figure 8c) relies on a rapidly rotating rotor to disrupt agglomerates directly, eliminating the need for grinding media while still achieving effective powder homogenization.

Like slurry-based processing, the dry mixing process is also crucial for the electrode properties and performance. Two key aspects of the dry mixing process are: mixing homogeneity and deagglomeration of particles. Mixing homogeneity refers to the uniform spatial distribution of all black mass components (e.g. AM, CA, and binder) throughout the powder blend, which is critical for ensuring consistent electrochemical performance and reproducibility. Deagglomeration involves the breakup of larger particle clusters into smaller, discrete particles, thereby improving the dispersion of materials and promoting effective interparticle contact. Together, these factors significantly influence the electrode's structural uniformity, electrical conductivity, and overall battery performance.

Scanning electron microscopy (SEM) is widely employed to assess the distribution of electrode components, particularly the degree of deagglomeration of conductive carbon and binder particles, as well as the overall homogeneity of their redistribution on the surface of the AM. SEM images provide visual evidence of how initial agglomerates of CA and binder are distributed across the AM surface. In the early stages of mixing, if the applied mechanical impact forces are insufficient, these agglomerates remain largely intact, leading to poor coverage and nonuniform distribution, as shown in Figure 9a. However, increasing the mixing intensity enhances the mechanical forces acting within the mixture, promoting the breakup of agglomerates. This results in a finer and more uniform dispersion of individual CB and binder particles across the AM surface, as illustrated in Figure 9b. In conclusion, uniform coverage of the AM surface by CA and binder ensures the

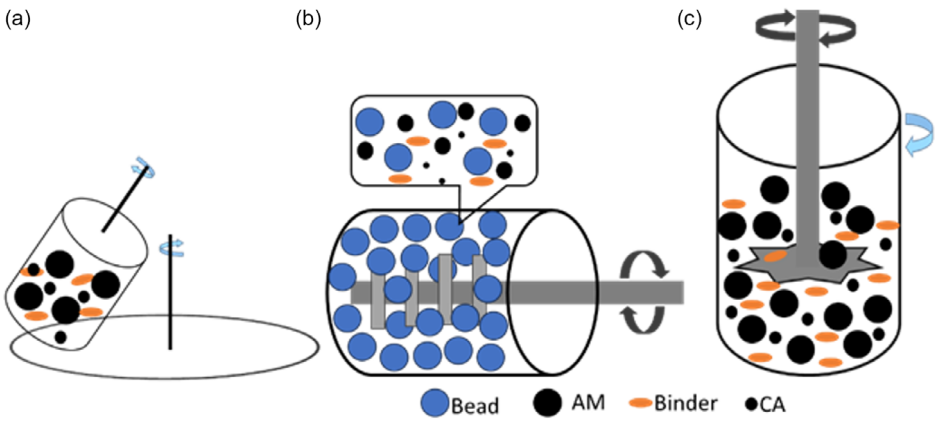

FIGURE 8 | Illustration of three common mixer types used for dry powder mixing in LIB electrode manufacturing: (a) planetary mixer, (b) bead mill homogenizer, and (c) high-shear mixer.

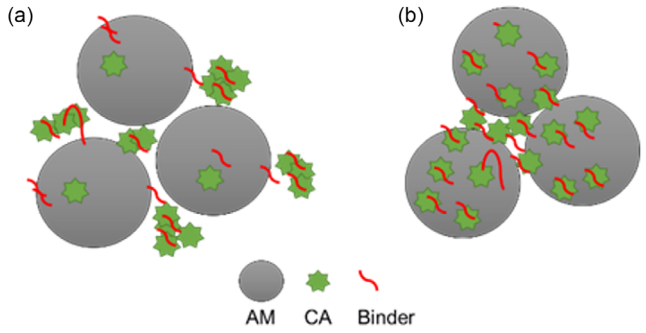

FIGURE 9 | Schematic illustration of powder mixtures (active material: AM, conductive additive: CA and binder) with (a) low homogeneity and limited deagglomeration and (b) high homogeneity with well-dispersed and deagglomerated components.

formation of continuous pathways, facilitating efficient ion diffusion and intercalation into the AM.

Mixing time and intensity are critical parameters that influence both the homogeneity of the mixture and the extent of particle deagglomeration in dry processing.

Tao et al. demonstrated that dry mixing duration significantly influences electrode morphology, component distribution, and PTFE fiber formation, which collectively affect the mechanical integrity and electrochemical performance of dry-processed electrodes [66]. Similarly, Gyulai et al. investigated the impact of dry mixing intensity (mixer revolution speed) by preparing three distinct mixtures: low revolution speed (low–intensity mixture: LIM), medium revolution speed (medium–intensity mixture: MIM), and high revolution speed (high–intensity mixture: HIM). Their study examined how increasing mixing intensity influences blend homogeneity, flow behavior, processability, and ultimately, the electrochemical performance of dry-laminated electrodes composed of $LiNi_{0.6}Mn_{0.2}Co_{0.2}O_2$ (NMC622) [67]. The SEM images of powder mixtures consisting of NMC622, Super C65 conductive carbon, graphite, and PVDF prepared at low (LIM, Figure 10a), medium (MIM, Figure 10b), and high revolution speeds (HIM, Figure 10c) illustrate that increasing the revolution speed progressively disrupts agglomerates and promotes the formation of a more homogeneous mixture [67].

Bulk electrical resistivity measurements of the powder mixtures are used to evaluate the degree of homogeneous distribution of CA within the AM matrix. Lower resistivity values indicate more effective deagglomeration and a more uniform dispersion of the conductive phase, which corresponds to enhanced electrical connectivity throughout the electrode.

The measured resistance R_s (Ω) and the corresponding specific bulk resistivity ρ (Ω·m) are determined using Ohm's law:

$$R_s = \rho \frac{L}{A} \rightarrow \rho = \frac{R_s A}{L} \tag{5}$$

where L (m) is the sample length and A (m^2) is the cross-sectional area. For practical measurement, the powder mixture is typically

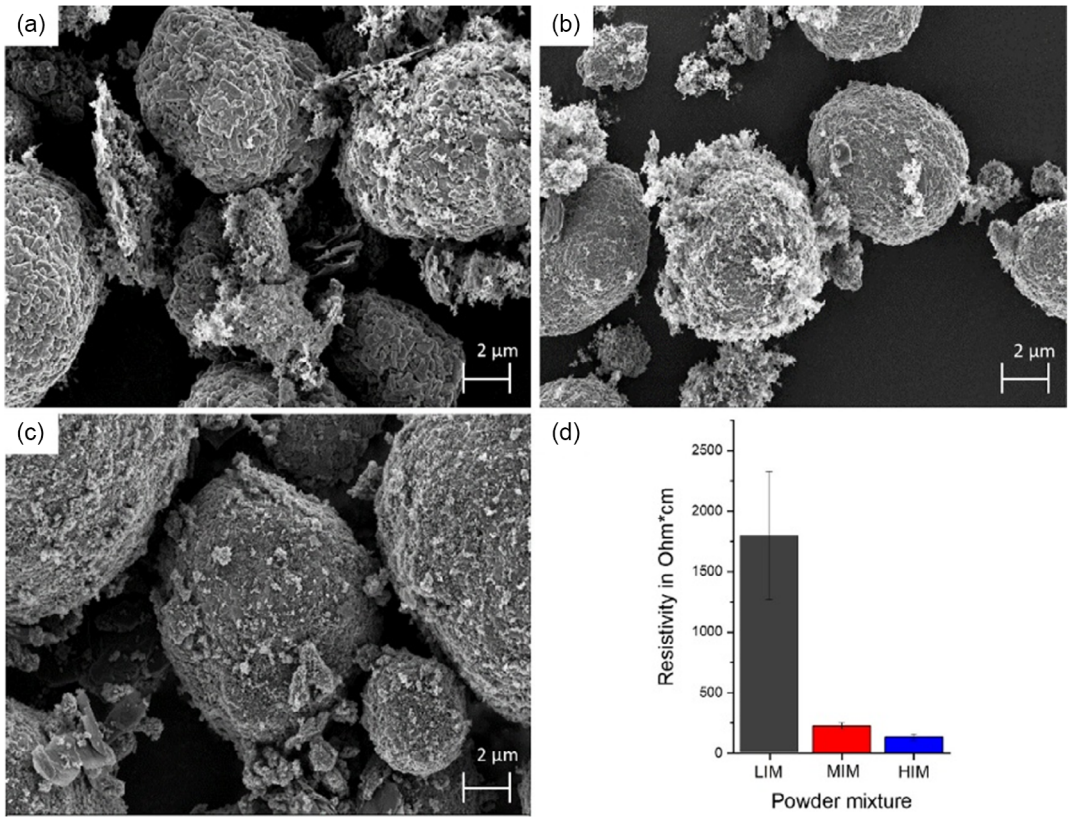

FIGURE 10 | Representative SEM images of the powder mixtures composed of NMC622, Super C65 conductive carbon, graphite, and PVDF at (a) the low revolution speed (LIM), (b) the medium revolution speed (MIM), and (c) the high revolution speed (HIM). (d) Electric resistivity of the corresponding powder mixture bulk at a normal load of 80 N and sample diameter of 24 mm [67]. Reproduced (Adapted) from Gyulai et al. Copyright 2023 The Authors published by the American Chemical Society, under the CC BY-NC-ND 4.0 license.

compacted into a cylindrical pellet with known L and A. Monitoring the bulk resistivity of the mixture at different stages of the dry-mixing process provides a useful metric for optimizing mixing conditions and improving powder homogeneity. Gyulai et al. also investigated the bulk electrical resistivity of three different powder mixtures composed of NMC622, Super C65 conductive carbon, graphite, and PVDF, prepared using a planetary mixer at varying revolution speeds (Figure 10d). Their results indicate that mixing at medium (MIM) and high (HIM) revolution speeds leads to lower resistivity values, suggesting a more homogeneous distribution of the conductive carbon (Super C65) and binder. This enhanced dispersion promotes the formation of an effective carbon–binder network, thereby ensuring improved electrical conductivity throughout the particle bed [67].

Thermogravimetric analysis (TGA) is a widely used analytical technique for determining the thermal stability and composition of materials by measuring weight changes as a function of temperature under a controlled atmosphere [68]. In the field of LIB electrode manufacturing, TGA serves as an effective tool for quantifying the relative content of individual components within electrode formulations, such as AMs, CA, and polymer binders [69]. During a TGA measurement, the electrode powder mixture (black mass) is gradually heated, causing the decomposition of thermally unstable components, typically organic binders like sodium CMC (Na-CMC) or PVDF, at different characteristic temperature ranges.

L. A. Gomez-Moreno et al. reported a rapid and straightforward method to quantify the graphite content in cathode black masses derived from $LiNi_{0.33}Mn_{0.33}Co_{0.33}O_2$ (NMC) and $LiCoO_2$ (LCO). The approach relies on TGA coupled with evolved gas analysis (TGA-EGA), which reveals a characteristic signal at approximately 450°C associated with the decomposition of trace amounts of PVDF [69]. Figure 11a presents the TGA profiles used to quantify the graphite content in cathode black mass mixtures composed of graphite/NMC, with the graphite fraction varying from 100% to 0%. As the NMC content increases, a greater amount of metal species (Ni, Co, and Mn) undergo reduction at elevated temperatures, resulting in a higher overall mass loss. By applying a linear fit between the graphite contribution and the corresponding mass degradation obtained from TGA, the graphite content can be expressed as a linear function of the measured mass loss, as shown in Figure 11b.

By analyzing the weight loss profile, the mass fractions of volatile and nonvolatile components can be accurately determined, enabling precise assessment of electrode composition and batch-to-batch consistency in dry or slurry-based processing.

Therefore, to evaluate the homogeneity and distribution of the binder within the powder mixture, TGA can be used to quantify the binder content by identifying its characteristic degradation temperature range within the mixture's TGA profile.

After the dry mixing process, which ensures a homogeneous and deagglomerated powder mixture, a further step is needed to "activate" the binder, i.e., to facilitate the formation of a cohesive network between the binder and the other powder components. This network has to effectively coat the AM particles, enabling proper electrode dough formation. The transformation of a dry, free-flowing powder mixture into a nonflowable, cohesive black mass is known as processability. In essence, processability reflects the mixture's readiness, indicating that the electrode materials have sufficient quality to form either a free-standing film or a coating on the current collector.

In this stage of processing, brittle or nondeformable electrode dough must be converted into granules using a high-shear mixer. The distribution of granule sizes serves as a quality indicator, analogous to slurry viscosity in wet electrode fabrication [39]. As depicted in Figure 2, the electrode precursors are mixed to form a viscous, dough-like mass that is later refined through mechanical grinding using a mixer or powder mill, ensuring the formation of electrode granules with uniform morphology and particle size distribution.

Depending on the type of binder and dry electrode manufacturing method, processability parameters such as mechanical forces of the mixers or thermal treatments have an impact on the modification of the rheological properties of the black mass. Mostly, a high-shear force is applied on the mixture to physically activate the binder and to form a cohesive network across the whole mixture.

In conventional wet electrode manufacturing, the impact of slurry rheology on electrode quality has been deeply investigated and assessed, whereas only a few studies have examined how the rheology of mixtures in the dry electrode manufacturing process affects processability. Viscosity cannot be used to characterize the rheology of a nonflowable, cohesive black mass. An alternative, effective option to optimize the electrode materials readiness or processability is the analysis of the mechanical torque of the blades or shafts during the mixing/kneading/extruding process

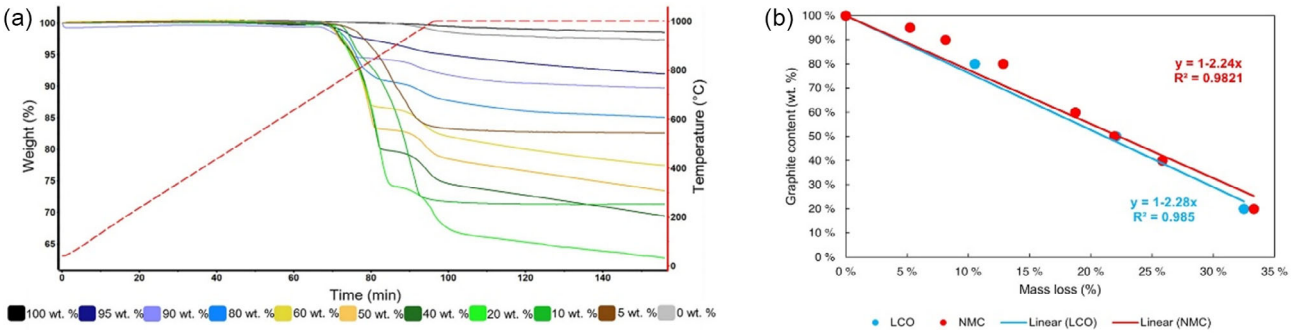

FIGURE 11 | (a) Thermogravimetric analysis (TGA) profiles of graphite/NMC mixtures with graphite contributions ranging from 100% to 0% and (b) linear fitting of TGA-derived mass degradation data used to quantify the graphite content in cathode black masses [69]. Reproduced (Adapted) from Gomez-Moreno et al., Copyright 2023. The Authors published under a Creative Commons CC BY license. Copyright 2023, Elsevier.

[39]. During the initial stages of processing by a mixer, kneader, or extruder, the interparticle friction increases, causing a rise in the equipment torque. During the process, this torque increases over time and reaches a maximum (peak) that marks the transition between a nonprocessable and processable state. The peak indicates that the binder is fully engaged in the mixing process. After the peak, torque begins to decline because the binder is redistributed or reshaped, facilitating the formation of a homogeneous and processable mixture.

Oh et al. developed a solvent-free process for fabricating dry electrodes composed of polytetrafluoroethylene (PTFE) binder, single-crystal NCM811 AM, and CB (Super P) and carbon nanotube (CNT) conductive agents. Initially, the AM and CA were blended in a powder mixer at a high revolution speed of 12,000/10 rpm. Subsequently, the PTFE binder was incorporated into the mixture under the same mixing conditions (12,000/10 rpm) to promote fibrillation and cohesion. The resulting cohesive composite was then kneaded at 10 rpm to form an electrode dough, which was subsequently transferred back to the powder mill for grinding and granule formation [39]. They followed the process by simultaneously monitoring the real-time changes of the kneader torque. They observed that the torque increased over time and after reaching a peak, it declined. They attribute this behavior to the transition of PTFE into a fibrous network, which enhanced its binding effect compared to its original particulate form [39]. A detailed discussion of the PTFE fibrillation treatment follows later in this section. Figure 12a demonstrates how kneading time influences the bulk morphology and microstructure of electrode doughs. Insufficient kneading leads to incomplete fibrillation of the PTFE binder, leaving unconverted primary particles, while excessive kneading produces a brittle, overworked dough. Both conditions prevent the formation of processable granular material. Figure 12b,c show real-time torque profiles, with an initial increase reflecting progressive PTFE fibrillation, followed by a decline indicating the completion of the transition to a fibrous network. Figure 12d shows that the required torque increases with higher binder content, indicating a greater mechanical resistance during processing as binder concentration rises.

The processability of dry powder mixtures during electrode fabrication is strongly governed by the chemistry and functionality of the binder. Each dry-processing method, such as dry spray deposition, melt extrusion, three-dimensional (3D) printing, powder compaction, or polymer fibrillation, requires a binder specifically tailored to its processing conditions to achieve cohesive, uniform, and mechanically robust electrode structures [25, 70–73].

However, this review does not seek to provide a comprehensive survey of all dry electrode manufacturing routes, which have

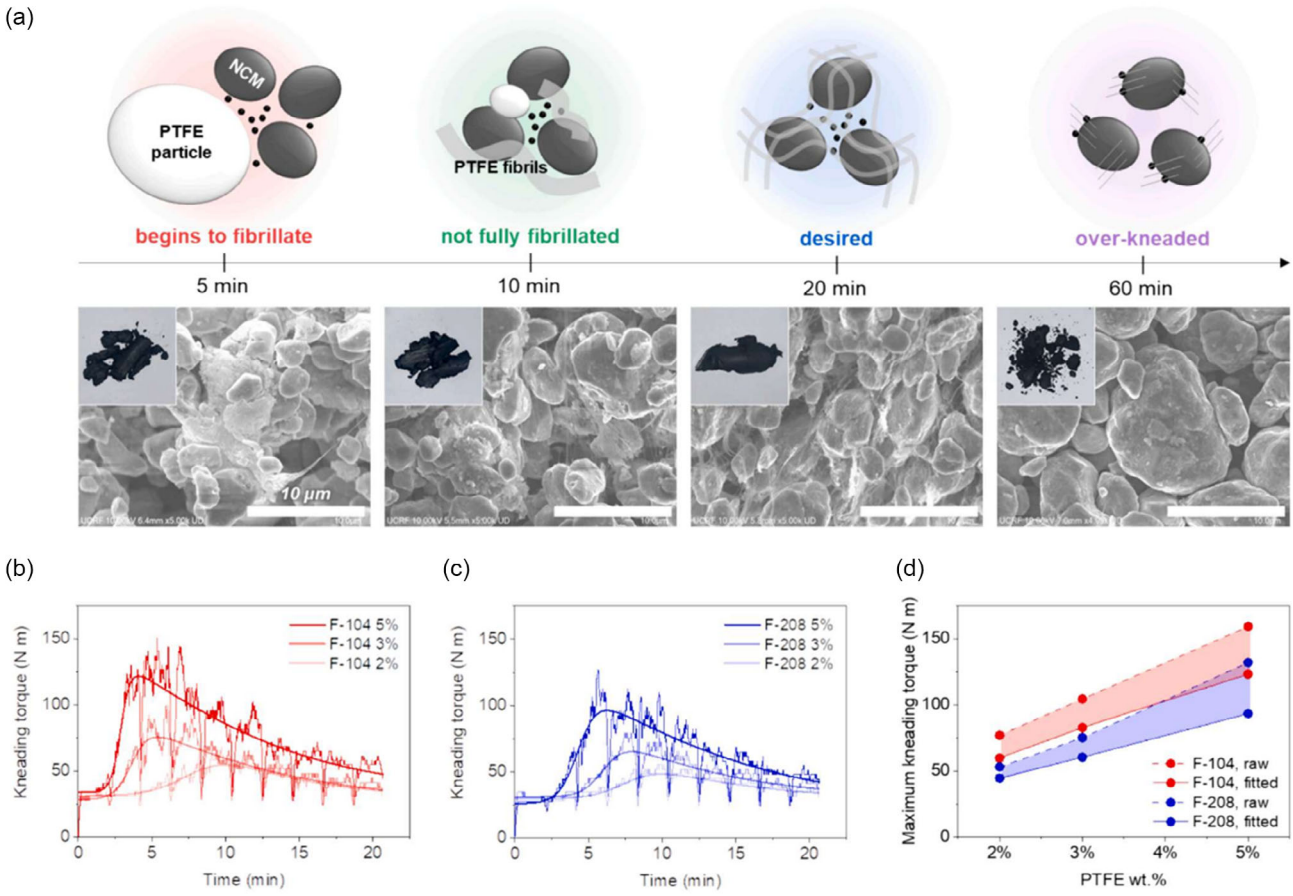

FIGURE 12 | Granule formation (kneading)—kneader—electrode dough. (a) Schematic diagram showing the fibrillation process of the PTFE binder with kneading time, photographs of the bulk shape, and SEM images of the microstructure of the electrode dough (PTFE F-208 2% wt%). (b,c) Real-time measurement results of the kneading torque change during kneading process. (d) Relationship between the amount of PTFE and maximum kneading torque by PTFE type [39]. Reproduced (Adapted) with permission, Copyright 2024, Elsevier.

been extensively discussed in several recent reviews [33, 38, 74]. Instead, it deliberately focuses on the mechanistic and process-level aspects that govern industrial scalability, particularly binder activation, powder rheology, processability metrics, and equipment–material interactions relevant to high-mass-loading, high–energy-density electrodes. By emphasizing these industrially critical factors, this review is intended to complement existing literature that primarily addresses materials chemistry or laboratory-scale demonstrations.

In contrast to wet electrode manufacturing, where solvents are utilized to disperse the binder throughout the slurry, thereby facilitating the formation of a cohesive network between AM particles and ensuring adhesion to the current collector, dry electrode processing relies on physical agents such as temperature and mechanical force to activate and distribute the binder. In other words, the mechanism relies on the thermomechanical activation of the polymer binder. Thermal treatment softens the polymer near its melting point, while simultaneously mechanical deformation, such as shear, tension, or compression, stretches and orients the polymer chains. This process induces fibrillation and may trigger phase transitions (e.g., from α- to β-phase in PVDF) [75], resulting in the formation of a robust, entangled fibrillary network. This network physically binds AM and conductive particles together and secures them to the current collector, all without the need for solvents. Such a mechanism enables the fabrication of cohesive and mechanically stable electrodes, making it highly suitable for scalable and environmentally friendly dry electrode manufacturing.

As illustrated in Figure 12a, fibrillation is a mechanically induced phenomenon in which polymer chains undergo alignment and elongation, resulting in the formation of fine, thread-like fibrils that interconnect particles and enhance mechanical integrity.

While many dry electrode scaling concepts have been proposed, PTFE fibrillation is the only mechanism that has been successfully translated to industrial-scale electrode production, as demonstrated by Maxwell Technologies for supercapacitors and later for LIBs [76]. This proven scalability is the primary reason PTFE fibrillation is emphasized in this review.

As established earlier, processability is ensured only when fibrillation yields a nonflowable cohesive mixture capable of stable film formation or uniform coating on the current collector. While the formation of a nonflowable cohesive state is a necessary condition, it is not, by itself, sufficient to ensure processability. In particular, the flowability range of the mixture reflects the extent of PTFE fibrillation achieved under specific shear conditions and processing times, but it should not be equated directly with processability. Rather, processability encompasses a broader set of criteria, including the ability of the fibrillated network to sustain deformation, granulation, and subsequent electrode shaping operations without mechanical failure. Flowability refers to the ability of a powder to undergo continuous, uniform flow under gravitational or imposed mechanical forces without agglomeration, segregation, or arching [77]. In the context of powder rheology, flowability is typically quantified using a combination of empirical and mechanical measurement approaches that capture different aspects of powder behavior [78]. One common method involves measuring the flow rate or discharge time of a defined mass or volume of powder through a standardized orifice, funnel, or rotary cylinder, with shorter discharge times indicating better flowability and lower interparticle cohesion. A more fundamental assessment is obtained through shear cell testing, where a consolidated powder bed is subjected to controlled normal and shear stresses to determine its yield behavior. From these measurements, a flow function is derived as the ratio between the applied consolidation stress and the unconfined yield strength, with higher flow function values corresponding to more freely flowing powders. In powder rheology, the flow function ($\mathrm{ff_c}$) is a dimensionless parameter obtained from shear cell measurements and is defined as [79]:

$$\mathrm{ff_c} = \frac{\sigma_1}{\sigma_c} \tag{6}$$

where σ_1 (Pa) denotes the major principal consolidation stress applied to the powder bed prior to shear testing, representing the normal stress under which the material has been compacted or stored and thus reflecting its degree of consolidation during handling, storage, or processing. The parameter σ_c (Pa) corresponds to the unconfined yield strength, defined as the stress required to induce failure of the powder bed once lateral confinement is removed. This quantity characterizes the internal cohesive strength of the consolidated powder and indicates its resistance to flow or structural collapse under self-weight.

In addition, flowability is often inferred from packing-based indices such as the Hausner ratio (HR) and Carr compressibility index (C_I), which are calculated from bulk (ρ_{bulk}) and tapped (ρ_{tapped}) densities ($\mathrm{Kg/m^3}$) and reflect the degree of interparticle friction and cohesion [80]:

$$\mathrm{HR} = \frac{\rho_{tapped}}{\rho_{bulk}} \tag{7}$$

$$C_I = \frac{\rho_{tapped} - \rho_{bulk}}{\rho_{tapped}} \tag{8}$$

Together, these methods provide complementary insights into powder flow behavior under both low-stress handling conditions and mechanically constrained processing environments.

Lischka et al. evaluated the flowability of dry-mixed NMC622/CB cathode materials using tapped density–based Hausner indices and ring shear cell measurements to capture powder behavior under unconfined and consolidated conditions [81]. All mixtures exhibited Hausner values above 1.4, indicating cohesive to very cohesive flow behavior, even prior to high-shear mixing. CB deagglomeration during mixing initially reduced bulk density and further degraded flowability, reaching a minimum at intermediate mixing times. With continued high-energy mixing, partial recovery of flowability was observed due to densification and restructuring of the CB network. Ring shear cell measurements confirmed these trends under applied normal stresses, demonstrating that the poorest flowability coincides with the lowest bulk density.

Upon the onset of PTFE fibrillation at any given mixing speed and processing time, the flowability of the powder mixture initially decreases due to the formation of a cohesive network, as reflected by an increase in the HR [81]. With continued mechanical input, a point of partial recovery in flowability may be reached, at which the HR begins to decrease. This phenomenon is illustrated in Figure 12a, where excessive kneading of the

cathode mixture results in an overworked structure characterized by a fragile, rigid, and excessively thin PTFE fibrillar network. Such over-fibrillation leads to a loss of cohesive integrity and a concomitant increase in flowability.

In conclusion, analysis of the flowability evolution provides a practical means to identify the optimal processing window, defined by mixing or kneading time and shear speed, required to produce a nonflowable yet cohesive mixture. As described previously, processability itself can be quantitatively assessed through real-time monitoring of the torque of the mixer, kneader, or extruder. The combined assessment of flowability and processability enables a comprehensive characterization of the rheological behavior of dry electrode mixtures. Together, these parameters capture both the low-stress flow response and the deformation behavior under processing conditions, thereby serving a role analogous to viscosity measurements in conventional wet electrode manufacturing.

Changes in powder flowability during dry electrode processing are governed by the thermomechanical activation of the binder, which promotes the formation of a cohesive mixture. Real-time monitoring of mixer, kneader, or extruder torque provides a practical means to track this transition and to identify the processing window required to achieve processability. As the binder composition undergoes thermomechanical activation, the initially free-flowing powder progressively transforms into a cohesive black mass. Among the available activation strategies, binder fibrillation is particularly effective at the industrial scale because it provides practical control over powder flowability and cohesion, enabling the formation of a mechanically stable and processable electrode [28, 39, 82].

The fibrillation behavior of a polymer is highly dependent on its molecular structure, degree of crystallinity, intermolecular forces, and processing parameters [83]. Polymers characterized by high molecular weight, linear chain architecture, and low van der Waals interactions are more susceptible to fibrillation due to reduced resistance to chain slippage and greater ease of molecular alignment under stress. Semicrystalline polymers such as PTFE exhibit a high tendency to fibrillate, attributed to their biphasic morphology in which crystalline domains confer mechanical strength while amorphous regions permit localized chain mobility. PTFE is capable of undergoing fibrillation when subjected to external mechanical forces [83]. Its molecular structure comprises a carbon backbone with each monomer unit bearing four fluorine atoms, forming strong carbon–fluorine bonds.

This robust bonding, combined with weak van der Waals interactions and a loosely packed molecular arrangement, facilitates the formation of an extended fibrous network. As a result, PTFE can fibrillate under relatively low SS, making it particularly suitable for applications requiring mechanical activation and structural reinforcement [31, 84]. Fibrillation typically occurs under shear, tensile, or elongational forces, at temperatures below the polymer's melting point but above its glass transition temperature to enable sufficient segmental motion without full melting. Additionally, high strain rates and uniaxial deformation enhance fibril initiation and propagation. These conditions collectively facilitate the formation of micro- to nanoscale fibrillar networks that play a pivotal role in determining the mechanical robustness and functional performance of dry-processed electrodes. The Maxwell-type dry battery electrode manufacturing process, developed by Maxwell Technologies and protected by a series of patents, is one of the most prominent approaches to dry electrode fabrication [85–87]. This method relies on the use of deformable polymer binders, such as PTFE, which possess high plasticity and the ability to form fibrils under applied shear forces [34, 66, 88]. These fibrils create a physically entangled network that effectively binds the AM and CA, resulting in a cohesive and mechanically robust electrode structure without the need for solvents.

As shown in Figure 13, the distinct fibrillation behaviors of PTFE and PVDF originate from fundamental differences in their molecular symmetry, crystallinity, and intermolecular interactions. PVDF is a partially fluorinated, semicrystalline polymer composed of $-CF_2-CH_2-$ repeat units, which introduce a permanent dipole moment along the polymer backbone due to the polarity contrast between C—F and C—H bonds. This polarity gives rise to strong dipole–dipole interactions in addition to London dispersion forces, leading to stabilized crystalline lamellae and restricted segmental mobility. Under applied shear or elongational stress, these intermolecular interactions impede chain rotation and slippage, limiting the ability of PVDF crystallites to unravel and form extended fibrillar structures. As a result, PVDF tends to undergo localized plastic deformation or brittle fracture rather than fibrillation, providing insufficient mechanical interlocking for robust cohesion in solvent-free dry electrode processing.

In contrast, PTFE is a fully fluorinated, semicrystalline polymer with a highly symmetric $-CF_2-$ backbone and no permanent dipole moment (Figure 13). The uniform distribution of highly electronegative fluorine atoms weakens intermolecular interactions between adjacent chains, facilitating chain mobility within crystalline domains. During solvent-free thermomechanical processing, such as warm mixing or kneading, PTFE crystallites can partially unravel as crystalline subdomains rotate, align with the applied stress field, and slide past one another. This behavior enables extensive fibrillation through the formation of micro- and nanoscale fibrils, resulting in a continuous, entangled network that provides mechanical integrity and cohesion to dry electrode mixtures. The kneading temperature and processing time critically govern the degree of fibrillation, which directly influences electrode strength and dimensional stability. In addition, insufficient fibrillation yields weak cohesion, whereas excessive fibrillation produces overworked, brittle networks.

These molecular- and crystalline-scale mechanisms are directly reflected in macroscopic processability indicators during dry electrode manufacturing. The progressive unraveling of PTFE crystallites and formation of a fibrillar network increases interparticle friction, producing a characteristic rise in mixer, kneader, or extruder torque. The torque maximum corresponds to the establishment of a fully percolated fibrillar network and marks the transition to a processable state. Continued mechanical input beyond this point results in torque reduction, signaling network homogenization or overfibrillation. In contrast, the limited crystallite mobility and suppressed fibrillation of PVDF lead to weaker torque signatures and a reduced processability window. This direct correlation between polymer crystal structure, intermolecular interactions, torque evolution, and processability explains why PTFE fibrillation remains uniquely suited for industrial-scale dry electrode manufacturing.

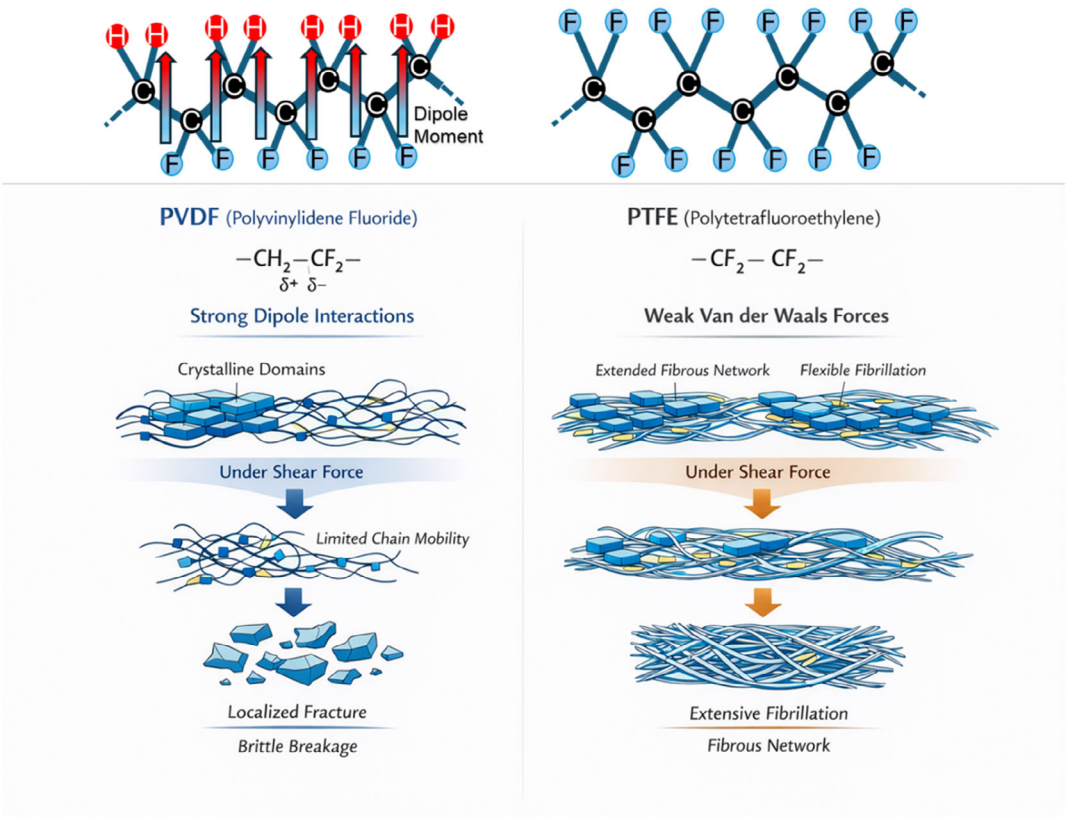

FIGURE 13 | Molecular structures and mechanical behaviors of PVDF and PTFE under shear force.

As previously mentioned, Oh et al. employed a kneading process to induce fibrillation of PTFE, thereby producing electrode doughs with the composition NCM811/PTFE/CB/CNT = 96/2.0/1.8/0.2 (wt%). The resulting dough was subsequently processed using a powder mill to refine it into submicron-sized electrode granules, with the objective of enhancing processability [39].

Therefore, PTFE not only improves mechanical integrity through its fibrillar network but also acts as a granulating agent during dry mixing, which is critical for roll pressing and subsequent electrode formation.

Activation of PTFE, i.e., transforming raw PTFE powder into a cohesive fibrillar network capable of binding electrode constituents, can proceed via two distinct routes: direct activation and indirect activation. In the direct route, PTFE undergoes fibrillation through mechanical or thermal stimuli, as previously described in this section, including the mixing–kneading protocol reported by Oh et al. [39]. In contrast, indirect activation entails premodifying the AM and CA mixture with specific processing aids that facilitate PTFE fibrillation without the need for high mechanical stresses typically imparted by kneaders or extruders. Thus, under appropriate conditions, PTFE can be activated to yield a processable powder blend for free-standing film fabrication while avoiding intensive mechanical treatment.

A patent by L. Zhong describes a method in which a flexible binder like PTFE is activated using specific additives and uniformly distributed onto active and conductive particles through high-speed mixing [89]. The resulting binder-coated particles are then compressed to form a self-supporting electrode film. Binder activation is achieved by incorporating a vaporizable solvent, comprising 20%–40% of the total electrode material, such as isopropyl alcohol (IPA), ethanol, or acetone, into the powder mixture. This processable mixture is subsequently pressed using a two-roll mill at a roll temperature of 120°C. The PTFE activation method described in L. Zhong's patent differs significantly from conventional PTFE fibrillation in both mechanism and processing requirements. While fibrillation relies on high mechanical stress, such as kneading or extrusion, to physically stretch PTFE particles into a fibrous network that binds components together, Zhong's approach achieves binder activation through the addition of solvents (e.g., IPA, ethanol, or acetone) and high-speed mixing with specific additives. This method eliminates the need for intense mechanical force, enabling more uniform distribution of the binder on active and conductive particles and simplifying the formation of free-standing electrode films. Although fibrillation provides strong mechanical integrity through a robust fibril network, the solvent-assisted activation technique offers a more scalable and less energy-intensive alternative for electrode fabrication.

AMs constitute the largest fraction in electrode formulations and, consequently, exert the most significant influence on the mechanical properties of the mixture. Therefore, achieving compatibility between the AMs and the targeted mechanical characteristics is crucial. When such compatibility is established, the binder can more effectively compensate for the absence of solvents in the dry electrode manufacturing process by forming a cohesive network that binds the particles together.

Reducing interparticle friction among AM particles enhances the binder's ability to transform the mixture into a processable material, ultimately allowing its deformation into a free-standing film. Lubrication of AM particles can substantially lower frictional

forces during mixing, thereby enabling the binder to fulfill its role without reliance on solvents. L. Zhong et al. have patented a dry electrode fabrication method that incorporates lubrication of the AM mixture, resulting in the formation of a free-standing electrode film [90]. In this approach, a conductive paste composed of a polymer additive, a liquid carrier, and a conductive material is prepared and employed as a lubricating agent. This paste is first mixed with the AMs to reduce interparticle friction, after which the binder is introduced. The lubricated mixture is subjected to shear forces and subsequently compressed to produce a free-standing film. The inclusion of a lubricating agent minimizes energy loss during shear mixing by reducing friction between AM particles. This enables the applied shear force to be more effectively directed toward activating the binder, thereby facilitating the formation of a cohesive network. The final pressing step further consolidates this network, yielding a mechanically stable and processable material suitable for free-standing electrode applications.

Several patents aimed at optimizing dry electrode manufacturing focus on thermomechanical activation of the polymer binder. This strategy exploits the temperature-dependent phase behavior and mechanical sensitivity of polymers, especially PTFE, enabling isolated binder particles to reorganize into a continuous structural framework that provides mechanical cohesion.

Typically, polymeric binders begin to deform upon exposure to elevated temperatures [91]. During thermal exposure, the polymer binder undergoes a physical transition known as thermal activation, whereby it softens and becomes prone to deformation and enlargement without fracturing. However, at excessively high temperatures, polymers may experience thermal degradation, characterized by the breakdown of polymer chains and subsequent deterioration of material properties [92]. To prevent such degradation and undesired rigidity, thermal activation is generally conducted at most a few degrees above the polymer's glass transition temperature. This approach ensures sufficient binder softening while mitigating the risk of thermal damage. K. Qiu et al. disclosed a patent involving a thermal activation process for dry electrode fabrication [93]. In this method, a mixture comprising the AM, CA, and binder was heated to approximately 70°C or higher. The mixture was then subjected to shear forces, resulting in the formation of an activated, cohesive structure, which was subsequently processed into a free-standing film using a roller press. The patent further introduced solvent activation, wherein a solvent such as acetone was applied to soften the thermally activated binder (e.g., PTFE), thereby minimizing the risk of rigidity and cracking. In summary, while exposure to high temperatures is necessary for thermal activation, the incorporation of solvents can effectively mitigate binder hardening. This dual activation strategy facilitates binder deformation and expansion without fracture, ultimately yielding a structurally stable and processable product.

Enhancing both mechanical and electrochemical properties, such as ductility, porosity, and ionic conductivity, is essential when selecting an appropriate binder or binder composition for dry electrode fabrication.

Despite its proven scalability through binder fibrillation, PTFE is increasingly subject to regulatory scrutiny as a per- and polyfluoroalkyl substance (PFAS), with ongoing legislative efforts in the United States and European Union aimed at restricting or phasing out fluoropolymers [94–96]. Together, these technical and regulatory constraints provide strong motivation for the development of cobinder or PTFE-reduced binder systems that retain the advantages of fibrillation-based processing while enhancing adhesion, ion transport, and mechanical robustness, and improving long-term sustainability and regulatory compatibility.

The use of cobinders can effectively satisfy the combined mechanical and electrochemical performance requirements. Duong et al. filed a patent on behalf of MAXWELL TECHNOLOGIES INC. for the production of dry electrodes intended for energy storage applications [97]. The electrode composition consists of graphite as the AM, CB as the CA, and various binders including PTFE, PVDF, polyethylene (PE), and mixtures such as PTFE/PVDF, PTFE/PE, and PTFE/polyethylene oxide (PEO). Figure 14 compares the electrochemical performance of lithium-ion half-cells assembled with anode electrodes produced by wet and dry processing techniques. Each electrode comprises graphite as the AM, CB as the CA, and binders of differing compositions. As illustrated in Figure 14a, although the use of PTFE as a binder

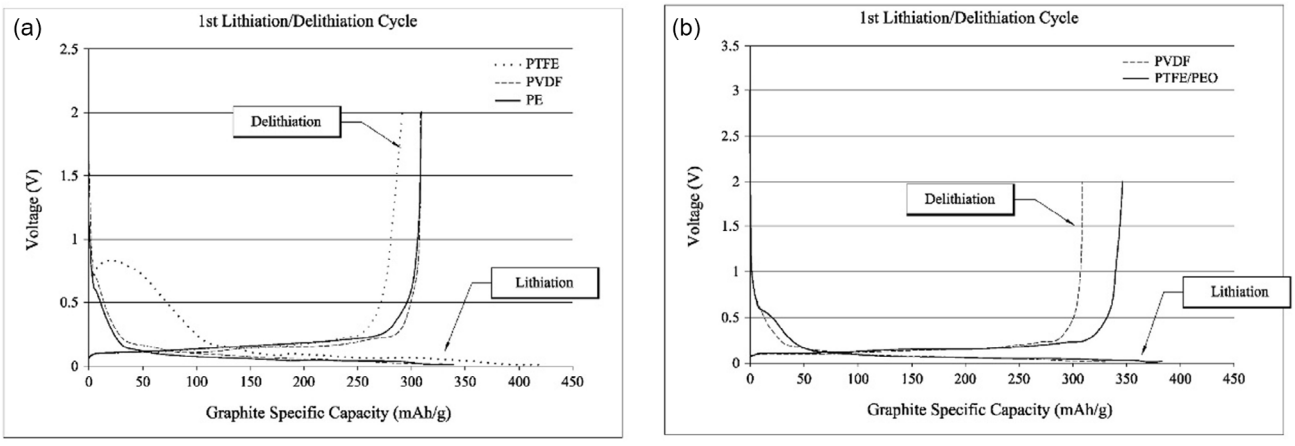

FIGURE 14 | Lithium-ion half-cell performance of graphite anodes formulated with carbon black and various binder systems, including PTFE, PE, PVDF, and PTFE/PEO. Specific capacities during the first lithiation and delithiation cycles are shown for: (a) dry-processed PE and PTFE electrodes compared with slurry-cast PVDF electrodes and (b) dry-processed PTFE/PEO electrodes compared with slurry-cast PVDF electrodes [97]. Reproduced (Adapted) from H. M. Doung, H. Feigenbaum, J. Hong, US Patent US010741843B2, 2015.

and its fibrillation process enabled the fabrication of ductile, free-standing dry electrodes, their electrochemical performance was not superior to that of PE-based dry-coated or PVDF-based wet-slurry electrodes. As shown in Figure 14b, incorporating PEO as a cobinder within the PTFE matrix improves the electrochemical performance of dry-fabricated graphite anodes, yielding higher performance than the PVDF-based wet-slurry counterpart.

The efficacy of the use of cobinders was also demonstrated in $LiNi_{0.8}Co_{0.1}Mn_{0.1}O_2$ (NMC811) cathodes. J. Kang et al. demonstrated a high-mass-loading dry cathode fabricated via a solvent-free process using NMC811 AM with a novel dual-binder system in which poly(acrylic acid)-grafted Na-CMC (PC) anchors to PTFE fibrils. By reducing PTFE content by over 70%, this "bollard-anchored" binder enabled fabrication of cathodes with loadings up to ~90 mg cm^{-2} (≈15.6 mAh cm^{-2}) exhibiting enhanced ionic conductivity, mechanical strength, and electrochemical performance compared to PTFE-only dry electrodes. These results highlight that tailored cobinder designs can significantly improve both mechanical integrity and functional performance in industrially relevant dry electrode manufacturing [98]. K. E. Sung et al. fabricated solvent-free dry cathodes composed of NMC811/CB/PTFE/polyacrylic acid (PAA) at a weight ratio of 96.8/1.2/1/1. The incorporation of the hydrogen-bonding cobinder PAA into the PTFE matrix significantly enhanced adhesion to the current collector and reduced interfacial resistance. As a result, the PAA/PTFE system exhibited improved rate capability and cycling stability, delivering higher discharge capacity and capacity retention compared with PTFE-only electrodes, demonstrating that cobinder strategies effectively overcome key mechanical and electrochemical limitations of PTFE-based dry electrode manufacturing [99].

3.1 | Industrial Perspective of Slurry Versus Dry Mixture

In conventional wet electrode manufacturing, from an industrial standpoint, slurry preparation is a mature and well-controlled process, benefiting from decades of optimization in rheology control, mixing hardware, and in-line quality monitoring [16]. The use of solvents enables efficient wetting of particles, reduction of interparticle friction and formation of a continuous binder network upon drying. This solvent-mediated homogenization is a primary reason why wet processing remains the industrial standard, particularly for high-throughput roll-to-roll manufacturing lines exceeding hundreds of meters per minute. However, slurry preparation also introduces nontrivial industrial penalties, including strict control of solid loading to maintain coatability, sensitivity to temperature and humidity, dependency on toxic and expensive solvents such as NMP and high downstream energy demand associated with drying and solvent recovery. These constraints increasingly limit the economic and environmental viability of wet processing [100], especially for thick, high-loading electrodes required for next-generation high-energy cells.

In dry electrode manufacturing, from an industrial perspective, dry powder mixing shifts the burden of homogenization from chemistry (solvents) to mechanics (shear, compression, and friction). Unlike slurry mixing, where viscosity can be continuously tuned via solvent content, dry mixing requires precise control of mixing intensity, residence time, particle morphology and surface properties, and binder deformability [66, 67, 81]. The absence of solvents removes drying-related bottlenecks and dramatically reduces energy consumption. However, it also introduces new scalability challenges, including agglomeration of CA, nonuniform binder distribution, sensitivity to mixer geometry, and operating conditions. As a result, powder mixing quality becomes a critical bottleneck for industrial dry electrode adoption, directly impacting electrical conductivity, mechanical integrity, and process yield.

In wet manufacturing, processability is governed by slurry rheology, primarily viscosity, yield stress, and shear-thinning behavior [41]. These parameters are directly linked to industrial coatability, enabling predictable transfer through pumps, pipelines, and coating heads.

At the factory scale, slurry rheology can be measured in real time, it is compatible with established quality-control protocols, and it directly correlates with coating uniformity and defect rates [58].

This well-established rheological framework is a major industrial advantage of wet processing, allowing rapid troubleshooting and high reproducibility across production batches. In contrast, dry electrode manufacturing involves nonflowable, cohesive mixtures, rendering conventional rheological descriptors such as viscosity meaningless. In dry processing, processability is instead defined by the mechanical readiness of the mixture, which is most effectively captured by real-time torque monitoring during mixing, kneading, or extrusion [39].

In industrial dry-mixing operations, torque monitoring provides a direct indicator of material processability: a rising torque reflects increased particle interaction during mixing, the appearance of a torque maximum signals effective binder activation, and the subsequent decline confirms the formation of a workable electrode mass. Practically, this torque maximum functions as an operational control point, analogous to target slurry viscosity, used to define the transition from loose powder to a manufacturable electrode precursor. Importantly, this torque-based criterion is equipment-dependent, requires process-specific calibration, and is currently less standardized than slurry rheology. The lack of universally accepted processability metrics remains a key barrier to industrial dry electrode scale-up, underscoring the need for in-line mechanical diagnostics. Table 2 presents a side-by-side comparison of wet and dry electrode manufacturing, highlighting the key differences in processability features and the practical metrics used to evaluate them. Wet processing is governed by well-established rheological parameters and benefits from standardized in-line monitoring and clearly defined quality-control windows. In contrast, dry processing assesses mixture readiness through mechanical response indicators, which remain under development and are often specific to the processing equipment. The table further highlights differences in industrial maturity and dominant process risks, contrasting coating-related defects typical of slurry-based routes with mixing- and binder-activation-related limitations inherent to solvent-free approaches.

From an industrial standpoint, the contrast between wet and dry material preparation is not incremental but structural. Wet processing benefits from chemical flexibility and mature control strategies but incurs high energy and environmental costs. Dry processing offers substantial sustainability and throughput advantages but demands new paradigms in process control, equipment design, and quality assurance. The choice between wet and dry

TABLE 2 | Comparison of processability features in wet versus dry electrode manufacturing.

Item	Wet processing	Dry processing
Governing parameter	Viscosity, yield stress	Torque, mechanical resistance
Measurement maturity	Highly standardized	Emerging
In-line monitoring	Widely implemented	Equipment-specific
Scalability	Proven	Under active development
Failure modes	Poor coating, cracking	Incomplete binder activation

processing is therefore not purely materials-driven, but strongly constrained by factory-level considerations, including energy pricing, regulatory pressure, equipment investment, and target electrode architecture.

3.2 | Binder Importance and Processing in Electrode Fabrication

Beyond its role as a passive adhesive, the binder acts as a process-enabling component that fundamentally determines whether an electrode formulation can be manufactured at scale. While both wet and dry electrode manufacturing rely on polymeric binders to provide mechanical integrity and adhesion, the processing mechanisms, performance constraints, and industrial requirements differ profoundly between the two routes.

In wet processing, binder processing is solvent-mediated and largely decoupled from mechanical deformation, whereas dry processing requires direct thermomechanical activation of the binder, making binder chemistry and molecular structure decisive factors for process success.

In conventional slurry-based electrode manufacturing, binders, such as PVDF, CMC, and SBR are dissolved or dispersed in a solvent prior to coating [16, 41]. Solvent-mediated binder processing provides three critical industrial advantages, such as uniform molecular-scale distribution of the binder, predictable rheological tuning through solvent content, and robust adhesion development during solvent evaporation. Upon drying, the binder precipitates and forms a continuous polymer network that binds AM and CA while anchoring the composite layer to the current collector. This mechanism is highly tolerant to variations in binder chemistry and molecular weight, which explains the broad applicability and robustness of wet processing across chemistries and electrode designs. However, this robustness is achieved at the cost of high-energy consumption, solvent management complexity, and limitations in thick-electrode fabrication due to binder migration and drying-induced stress gradients [101].

In dry electrode manufacturing, solvent-mediated binder processing is entirely absent. Instead, binder activation relies on mechanical deformation, thermal softening, or a combination of both, requiring polymers that can undergo controlled deformation without fracture. Among commercially available binders, PTFE has emerged as the most widely adopted binder for dry electrode manufacturing, owing to its exceptional fibrillation capability under shear and tensile stress [34].

In contrast to PTFE, PVDF exhibits limited fibrillation capability under dry-processing conditions, despite its widespread use in wet processing. As a result, PVDF alone is generally unsuitable as a primary binder for solvent-free dry electrode manufacturing.

This mechanistic distinction explains why binder selection is not transferable between wet and dry processing, and why dry manufacturing demands binders explicitly designed for thermomechanical activation.

To overcome the intrinsic limitations of single-binder systems, industrial dry electrode manufacturing increasingly relies on binder engineering strategies, including PTFE-based primary binders for mechanical integrity, secondary cobinders (e.g., PEO, PE, CMC, PAA) to improve ionic transport and ductility, and controlled thermal activation near the binder glass-transition temperature [97–99]. Table 3 summarizes the contrasting binder requirements for industrial wet versus dry electrode manufacturing. In wet processing, binder activation relies on solvent dissolution, requiring relatively low polymer chain mobility and no fibrillation capability, allowing for a broad selection of binder chemistries and offering high industrial robustness due to mature processing methods. Conversely, dry processing demands thermomechanical activation of binders with high chain mobility and essential fibrillation ability to form cohesive networks without solvents. This narrows the binder options and presents ongoing challenges in achieving comparable robustness, highlighting binder chemistry as a critical design parameter for scalable dry electrode production.

This distinction underscores that binder chemistry is a first-order design parameter for dry electrode manufacturing, rather than a formulation detail.

In industrial dry electrode manufacturing, binder processing must be verified in real time, as incomplete fibrillation directly leads to poor film formation, delamination, and inconsistent electrochemical performance. Torque monitoring during mixing and kneading has therefore emerged as a critical in-line diagnostic, serving as the dry-processing analog of slurry viscosity in wet manufacturing. The identification of a characteristic torque maximum provides a reproducible indicator of binder activation and

TABLE 3 | Binder requirements for industrial wet versus dry electrode manufacturing.

Requirement	Wet processing	Dry processing
Processing mechanism	Solvent dissolution	Thermomechanical activation
Chain mobility needed	Low	High
Fibrillation capability	Not required	Essential
Binder diversity	Broad	Limited
Industrial robustness	High	Developing

mixture readiness, enabling process control in continuous manufacturing environments.

4 | Industrial Perspective of Coating and Drying Steps

In wet electrode manufacturing, once the slurry meets the targeted rheological window, it is transferred to the coating stage. As discussed in Section 3, during coating, shear is imposed through pumping, transfer lines, and the coating head, allowing the slurry to overcome its yield stress and spread uniformly onto the current collector. Below this threshold, the slurry behaves elastically, whereas exceeding it enables continuous flow and film formation [55]. Consequently, the coating line must deliver sufficient shear to ensure reliable spreading and defect-free deposition. Beyond rheology, coating outcomes are also governed by physical parameters such as coat thickness, areal loading, and surface quality, all of which directly influence electrode performance and manufacturing robustness [102].

As shown in Figure 15, the slurry can be spread on a current collector using various methods, including doctor blade coating, slot-die coating, and comma bar coating. In doctor blade coating, a blade spreads the slurry onto a moving metal foil, such as aluminum for cathodes or copper for anodes. Slot-die coating uses a precise nozzle to evenly deposit the slurry onto the collector, ensuring better thickness control.

In comma bar coating, a comma-shaped bar with a curved leading edge applies the slurry to the current collector, providing a uniform coating. The geometry of the doctor blade and comma bar controls the slurry volume deposited on the substrate, whereas slot-die coating is preregulated, meaning the slurry volume applied to the substrate is determined by the pump flow rate. The slot-die coating technique is commonly used in industrial electrode production [14].

LIB electrode coating is a vital process step that directly affects electrode quality, battery performance, and production efficiency [103, 104]. However, this step poses numerous challenges that must be carefully managed to ensure consistent, high-performance outcomes [105]. One major issue is slurry uniformity, since inadequate mixing or poor dispersion of AMs, binders, and CA can lead to nonuniform coatings, ultimately compromising electrochemical performance and cycle life [106]. Controlling coating thickness is equally essential, as even minor variations can result in uneven current distribution, capacity imbalances, and reduced energy density [107]. The push toward high-loading electrodes, which is needed to increase LIB energy density, adds complexity, as thicker coatings are more prone to cracking and mechanical failure. Additionally, defects such as edge beading, streaks, or pinholes, often caused by suboptimal coating parameters, can degrade mechanical integrity, increase internal resistance, or even trigger short circuits [108, 109]. Adhesion to the current collector (typically aluminum for cathodes and copper for anodes) must be uniform and strong; otherwise, delamination during drying or cycling may occur. Furthermore, maintaining coater speed and web tension at high-throughput rates is technically demanding and can lead to coating irregularities, wrinkles, or tearing if not carefully controlled [103]. The choice of solvent (e.g., NMP or water) significantly affects slurry rheology and drying behavior, and poor solvent compatibility can lead to instability and inadequate film formation [41]. Scalability and repeatability also pose challenges, as processes optimized at lab or pilot scales often fail to translate effectively to large-scale production. Lastly, environmental and safety concerns, especially with volatile solvents like NMP, require robust handling systems and regulatory compliance to mitigate health and operational risks.

The current collector foil coated by the slurry passes through a drying oven to evaporate the solvent, leaving a solid layer of composite material (AM, conductive carbon additive and binder), i.e. the so-called black mass. The electrodes are thoroughly dried to remove any residual solvent, typically in a convection oven or under vacuum. This step is critical to avoid impurities that might degrade battery performance or impact safety.

Electrode drying is a fundamental stage in the wet process that significantly impacts battery performance, process consistency, and overall production cost [104]. This step presents several technical challenges that must be carefully addressed to ensure optimal results [110]. Drying uniformity is a primary concern, and uneven drying across the electrode surface or through its thickness can cause irregular distribution of binder and CA, leading to weak adhesion, cracking, nonuniform porosity, and reduced electrochemical performance [111–115]. During solvent evaporation, capillary and diffusion-driven binder migration toward the electrode surface can create uneven binder distribution and localized weak points, shortening battery lifespan [113, 114]. Thick coatings, while desirable for achieving high-energy density, are more sensitive to drying variations and prone to defects such as

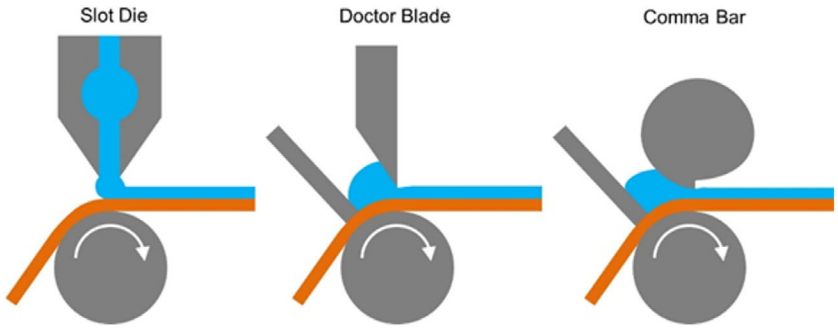

FIGURE 15 | Schematic representation of slot-die, doctor-blade, and comma-bar coating geometries integrated into a roll-to-roll coating system [102]. Reproduced (Adapted) from C. D. Reynolds et al., Copyright 2021. The Authors published under a Creative Commons CC BY license. Copyright 2021, Elsevier.

cracking, delamination, and binder migration [115]. While faster drying can increase throughput, it often worsens coating quality. Indeed, it might lead to binder migration, especially in the case of PVDF-based thick electrodes, resulting in mechanical instability, delamination from the current collector, and overall structural inconsistency [100].

Solvent recovery and environmental management also play a vital role, particularly for NMP-based systems. Recovering this toxic and expensive solvent requires advanced equipment such as condensers and scrubbers, which significantly increase energy consumption and operational complexity [100]. Scaling up the drying process from laboratory to industrial scale introduces additional challenges, as maintaining consistent conditions such as temperature, airflow, and humidity becomes more difficult, often leading to greater variability in electrode quality. Material-specific drying requirements also complicate process optimization, for example, silicon-based anodes and high-nickel cathodes each demand tailored drying protocols to maintain structural and electrochemical integrity [116, 117].

Lastly, energy consumption remains one of the most pressing concerns, as drying is among the most energy-intensive steps in LIB manufacturing, directly contributing to both operational costs and environmental footprint if not optimized effectively [118]. Large convection ovens with residence lengths of tens of meters are required to ensure complete solvent evaporation at high web speeds, and solvent recovery systems, particularly for NMP, significantly increase both capital expenditure (CAPEX) and operating expenditure (OPEX) [100, 118]. Industrial analyses consistently report that electrode drying alone accounts for approximately 30%–50% of the total energy consumption in slurry-based Li-ion battery manufacturing, making it one of the dominant contributors to manufacturing cost and environmental footprint [104].

In slurry-based electrode manufacturing, coating and drying represent two of the most capital- and energy-intensive steps, imposing fundamental constraints on throughput, electrode architecture, and overall manufacturing cost, while pilot-scale studies have quantitatively demonstrated that the combined operating conditions of these stages directly govern the final physical properties and electrochemical performance of LIB electrodes [100, 104]. Román-Ramírez et al. systematically demonstrated that parameters, such as comma bar gap, web speed, coating ratio, drying temperature, and drying air speed significantly affect key electrode properties, including thickness, mass loading, and porosity, which in turn govern gravimetric and volumetric capacity as well as rate capability [104]. Their design-of-experiments approach revealed that suboptimal coating and drying conditions can lead to nonuniform microstructures that deteriorate AM utilization and cycle life, highlighting the need for tight control of these process steps in industrial production. This work underscores that coating-drying interactions are not independent; instead, they jointly determine microstructural evolution and electrochemical behavior, reinforcing the importance of integrated process optimization in conventional slurry-based manufacturing.

Dry electrode manufacturing fundamentally eliminates coating-related rheological constraints and removes solvent evaporation and recovery from the process flow. From an industrial perspective, this translates into a substantial reduction in process energy demand, factory footprint, and equipment complexity, while enabling shorter production lines and lower fixed costs. However, the absence of a liquid phase shifts the primary manufacturing constraint upstream, from coating and drying to powder processability and binder processing. Uniform film formation in dry processing relies on achieving a nonflowable yet deformable cohesive mixture capable of being calendered or roll-pressed into a dense electrode layer. Accordingly, process control in dry electrode manufacturing is no longer governed by viscosity or drying kinetics but by mechanical indicators such as mixing torque during kneading or extrusion [39].

From an industrial standpoint, the contrast between slurry-based and dry electrode manufacturing is therefore most pronounced at the coating and drying stages. Slurry processing benefits from standardized control strategies and broad binder compatibility but incurs high-energy consumption, large CAPEX requirements, and solvent-related regulatory and environmental burdens. Dry processing removes these constraints entirely, offering compelling advantages in energy efficiency and line simplification, but demands new paradigms in mechanical process control, binder design, and in-line diagnostics. The choice between these manufacturing routes is thus not solely materials-driven, but fundamentally shaped by system-level considerations including energy pricing, CAPEX/OPEX trade-offs, regulatory pressure, and scalability requirements.

5 | Calendering Step in Electrode Manufacturing

In conventional wet electrode manufacturing, the calendering process involves passing dried electrodes through a set of heated rollers under controlled pressure [119]. Calendering alters the mechanical properties and deformation behavior of LIB electrodes and introduces several technical challenges that must be carefully managed. This process primarily affects electrode porosity, thickness, adhesion to the current collector, mechanical integrity, and charge transport properties [119]. Wang et al. demonstrated that the calendering compression rate not only determines the macroscopic mechanical characteristics but also significantly affects the microstructure of the electrode coatings, including porosity and pore size distribution [120]. Achieving optimal electrode porosity is essential, as low porosity can impede ion transport and increase internal impedance, whereas high porosity may decrease volumetric energy density and weaken mechanical stability [121]. The coating density of the electrode plays a significant role in determining battery performance, and achieving uniform density across the electrode sheet is essential for consistent electrochemical behavior. Optimizing the compression process can effectively tailor both density and porosity, which critically influence the overall electrochemical performance of the cell [119, 122]. Thickness precision is also crucial, as even minor deviations can lead to stacking issues, suboptimal contact pressure, and inconsistent cell performance. Adhesion to the current collector is another critical parameter, as improper pressure settings may result in delamination or poor interfacial contact, increasing internal resistance and the risk of mechanical failure during operation. Mechanical integrity may be compromised by excessive compression, which can create microcracks in AMs or disrupt the binder matrix, ultimately reducing cycle life. Conversely, if calendering pressure is too low, weak

interfacial contact may occur, increasing internal resistance and leading to delamination under cycling. Additionally, particle deformation during compression can fracture or reshape AMs, particularly in high-energy-density chemistries such as silicon-based anodes or high-nickel NMC cathodes, negatively affecting long-term performance and safety.

The calendering response varies by electrode type: graphite anodes, being more elastic, are especially sensitive to pressure, while cathodes can tolerate higher loads but are more prone to cracking [123]. Equipment-related factors such as roller alignment and surface quality also influence outcome, and misaligned or worn rollers may apply uneven pressure, resulting in surface defects and nonuniform properties. Moreover, heat generated during calendering from friction can alter binder behavior or degrade temperature-sensitive materials if not properly controlled [119]. As the industry advances toward thicker, high-loading electrodes to achieve higher energy densities, calendering demands even greater precision and process optimization to preserve structural integrity and electrochemical performance.

In dry electrode manufacturing, the processable powder mixture is passed through heated rollers that simultaneously apply mechanical pressure and thermal energy, promoting particle fusion and forming a cohesive, mechanically robust film [124]. The calendering process transforms the dry processable powder mixture into a self-supporting electrode film via mechanical compression and densification. This resultant film is then laminated onto a current collector, such as aluminum foil for the cathode or copper foil for the anode.

The calendering process is essential in dry electrode manufacturing, as it enables several key transformations: the development of a fibrillar network when fibrillizable binders such as PTFE are used, the compression and densification of the processable powder mixture to lower porosity and increase bulk density, and the lamination of the resulting free-standing film onto the current collector.

In both wet and dry electrode fabrication processes, calendering significantly influences the electrode's microstructure by affecting its density, porosity, adhesion, thickness, wettability, charge transport properties, and particle distribution [119]. Consequently, in a dry-processed electrode, calendering serves as an effective means of controlling the microstructure of both free-standing films and the final laminated electrode. To achieve more precise control over the microstructure, the calendering process can be optimized by systematically adjusting parameters such as roller temperature, applied pressure, surface roughness, and rolling speed, thereby tailoring the electrode properties to meet specific requirements [67].

During dry electrode fabrication, the frictional interaction between the calendering machine rolls and the processable mixture plays a crucial role in the formation of a free-standing film. Therefore, specific calendering configurations such as rolls with varying surface morphologies and material properties can be employed to modulate friction, thereby promoting internal shearing within the powder and facilitating film formation.

Furthermore, differential roll speeds are essential to induce shear planes within the mixture [67]. By increasing the relative velocity between adjacent particles, shear deformation within the powder is enhanced, contributing to the successful development of a free-standing film.

Lamination constitutes the final stage of the calendering process in dry electrode manufacturing, wherein the fabricated free-standing film is applied onto the current collector with a controlled thickness by adjusting the gap between the calender rolls [32]. Moreover, the current collector is typically precoated with a thin, conductive, and cohesive layer to enhance the mechanical integrity and electrical performance of the resulting electrode.

Overall, calendering serves as a microstructure-tuning step in slurry-based electrode manufacturing, where its primary function is to compensate for coating and drying-induced heterogeneities by adjusting density, porosity, and adhesion. In dry electrode manufacturing, by contrast, calendering is a process-enabling operation that directly governs film formation, binder activation, and lamination in a single step. This fundamental difference shifts the role of calendering from a corrective operation to a central manufacturing bottleneck, placing greater emphasis on mechanical control parameters such as pressure, friction, temperature, and roll kinematics. Consequently, while both processes rely on calendering to achieve electrochemical performance targets, dry electrode manufacturing demands tighter integration between material design and calendering mechanics, reinforcing its distinct process logic relative to conventional slurry-based routes.

6 | Summary and Outlook

As global demand for advanced energy storage systems intensifies, the optimization of LIB electrode manufacturing becomes increasingly critical. Conventional wet manufacturing remains the industry standard due to its well-established infrastructure, predictable processing, and compatibility with diverse chemistries. It ensures homogeneity and strong electrode adhesion but suffers from significant environmental and economic drawbacks, primarily related to solvent use, energy-intensive drying, and limitations in thick electrode fabrication.

Dry electrode manufacturing offers a transformative alternative, addressing many of these concerns by eliminating solvent use and associated drying processes. This not only reduces environmental impact and operational costs but also simplifies production workflows and facilitates the fabrication of mechanically robust thick electrodes. Furthermore, dry processing aligns well with emerging high-capacity materials that require improved structural cohesion and precise porosity control. Nevertheless, it introduces its own challenges, such as binder fibrillation mechanics, difficulties in achieving uniform component dispersion, complex processability verification, and high initial equipment costs. The limited industrial adoption of dry methods is largely due to the need for novel equipment, real-time rheological monitoring tools, and optimized binder activation strategies.

This review outlines the key opportunities, limitations, and challenges associated with wet and dry electrode manufacturing for LIB production that can be summarized as follows:

- Material Homogeneity: In wet electrode manufacturing, the use of solvents enables the formation of a homogeneous slurry of electrode materials at both laboratory and industrial scales. In contrast, dry electrode manufacturing relies entirely on the mixer's ability to achieve a uniform distribution of materials without solvents. Therefore, industrial implementation of dry electrode processing requires

thorough investigation of mixing technologies, particularly with regard to the mixing homogeneity, deagglomeration, and uniform dispersion of binder particles during the blending process.

- Rheological Characterization and Processability: In solvent-based slurries, rheological measurements are well-established and provide reliable data on viscosity, which directly correlates with processability. In dry electrode manufacturing, forming a cohesive black mass through the thermomechanical binder activation is essential but insufficient as the sole indicator of processability. A mixture is considered processable only when the binder is fully activated and uniformly integrated into a cohesive network that renders the material deformable and suitable for film formation or current collector coating. Consequently, the equipment used, such as mixers, kneaders, or extruders, should be equipped to monitor parameters like torque, which change in response to the rheological state of the cohesive mixture. Beyond materials selection and process flow, factory-level implementation of dry electrode manufacturing will require the development of standardized in-line diagnostics and acceptance criteria. Unlike wet processing, where viscosity and yield stress provide transferable quality metrics, dry processing lacks universally defined indicators of mixture readiness and manufacturability. Establishing equipment-agnostic correlations between torque signatures, thermal history, and resulting electrode microstructure will be essential to enable reproducibility across different mixers, kneaders, and calendering systems.
- Drying Challenges and Material Integrity: During the drying phase of wet electrode manufacturing,the presence of solvents often introduces complications, including binder redistribution, particle agglomeration, poor adhesion, cracking, nonuniform porosity, and degraded electrochemical performance. These issues are particularly pronounced in thick cathodes or water-based anodes. In contrast, dry electrode processing, which eliminates the need for high solvent content, effectively minimizes these challenges and supports more consistent electrode quality.
- Calendering Functions and Equipment Demands: In dry electrode manufacturing, the calendering step serves a dual purpose: it transforms the processable powder blend into a dense, cohesive. free-standing electrode and laminates it onto a current collector. In wet processing, calendering is primarily used to compress the dried slurry-coated electrodes, reduce porosity, enhance particle contact, and improve adhesion and energy density. While conventional wet electrodes can be calendered using standard rollers, dry-processed electrodes often require rollers with specialized surface properties and differential speeds to achieve optimal film formation and structural integrity.
- Binder Processing as the Core Differentiator: Binder processing represents the most fundamental mechanistic difference between wet and dry electrode manufacturing. While wet processing externalizes complexity through solvents, dry processing internalizes it within binder chemistry and mechanical activation. Successful industrial adoption of dry electrodes therefore, hinges on binder systems explicitly designed for thermomechanical activation, rather than on direct translation of wet-processing formulations.

Another critical but underexplored aspect is the interdependence between dry electrode processing and downstream cell assembly steps, including stacking, winding, and electrolyte infiltration. Dry-processed electrodes often exhibit distinct pore architectures and surface chemistries compared with slurry-cast counterparts, which can influence wetting kinetics, gas evolution, and formation behavior. Systematic integration studies linking dry electrode microstructure to cell-level manufacturing robustness remain scarce and represent an important opportunity for future work.

From a sustainability and regulatory standpoint, binder selection in dry electrode manufacturing will increasingly be shaped by environmental policy rather than performance alone. The potential classification of PTFE as a regulated PFAS compound introduces strategic uncertainty for long-term industrial adoption. This reinforces the need for binder architectures that reduce fluoropolymer content, enable partial replacement through cobinder strategies, or leverage alternative thermomechanically activatable polymers while preserving processability.

Finally, the transition to dry electrode manufacturing necessitates a shift in equipment design philosophy. Most current implementations adapt legacy wet-processing hardware, whereas fully realizing the advantages of dry processing will require purpose-built mixers, calendering systems, and laminators optimized for friction-dominated, nonflowable materials. Codevelopment of materials, process metrics, and hardware will therefore be a defining requirement for scaling dry electrode technologies from pilot lines to high-throughput industrial production.

Moving forward, integrating dry processing into mainstream LIB production will require addressing these technical and scalability barriers. Advances in cobinder chemistry, thermal and mechanical activation mechanisms, and real-time torque or morphology-based quality control will be vital. Furthermore, hybrid approaches, combining the strengths of both wet and dry techniques, may present a practical pathway for balancing performance, sustainability, and economic viability.

Importantly, many of the insights gained from dry electrode research in LIBs are directly transferable to other battery chemistries (e.g., sodium ion batteries) and supercapacitor manufacturing. Supercapacitors, which rely on highly conductive porous electrodes and minimal binder content, can greatly benefit from solvent-free processing that enhances interparticle connectivity and electrode uniformity. The adoption of dry coating and fibrillation-based binder strategies may therefore accelerate the development of next-generation high-power, environmentally sustainable supercapacitors.

By fostering innovation in process design, materials engineering, and in-line monitoring, both academic and industrial stakeholders can unlock the full potential of dry electrode manufacturing in shaping the next generation of LIBs.

Acknowledgments

This work has been carried out under the National PhD program in SUSTAINABLE MATERIALS, PROCESSES AND SYSTEMS FOR ENERGY TRANSITION at the Department of Chemistry "Giacomo Ciamician", Alma Mater Studiorum University of Bologna, and Department of Applied Science and Technology (DISAT), Politecnico di Torino. S. M. acknowledges COMAS SPA for cofunding the PhD grant.

F. S. acknowledges DiGreen: a digital and chemical approach for green recycling of Li-based batteries" funded by the European Union - Next Generation EU, Missione 4 Componente 1 Project CUP J53D23008790006, and MOST—Sustainable Mobility Center project, funded by the European Union Next-Generation EU (PIANO NAZIONALE DI RIPRESA E RESILIENZA (PNRR) e MISSIONE 4 COMPONENTE 2, INVESTIMENTO 1.4 e D.D. 1033 17/06/2022, CN00000023. The authors gratefully acknowledge Mauro Serafin and Elisa Maruccia from COMAS SpA for the fruitful discussions on industrial-scale dry coating processes.

Open access publishing facilitated by Universita degli Studi di Bologna, as part of the Wiley - CRUI-CARE agreement.

Funding

This study was supported by European Commission (J53D23008790006 and CN00000023).

Conflicts of Interest

The authors declare no conflicts of interest.

Data Availability Statement

Data sharing is not applicable to this article as no new data were created or analyzed in this study.

References

1. N. T. M. Balakrishnan, A. Das, N. S. Jishnu, et al., "The Great History of Lithium-Ion Batteries and an Overview on Energy Storage Devices," *Materials Horizons: From Nature to Nanomaterials, Springer Nature* (2021): 1–21.

2. M. Winter and S. Passerini, "Lithium ion batteries as key component for energy storage in automotive and stationary applications," *In Proceedings of the 2011 IEEE 33rd International Telecommunications Energy Conference (INTELEC), Amsterdam*, (The Netherlands, 2011): 9–13 October.

3. S. D. Wankhade and B. R. Patil, "Leveraging Storage Batteries for Sustainable Green Energy Harvesting: From Li-Ion Perspective," *International Journal of Membrane Science and Technology* 10 (2023): 257–277.

4. Md D. Ahmed and K. M. Maraz, "Revolutionizing Energy Storage: Overcoming Challenges and Unleashing the Potential of Next Generation Lithium-Ion Battery Technology," *Materials Engineering Research* 5 (2023): 265–278.

5. H. C. Hesse, M. Schimpe, D. Kucevic, and A. Jossen, "Lithium-Ion Battery Storage for the Grid—A Review of Stationary Battery Storage System Design Tailored for Applications in Modern Power Grids," *Energies* 10 (2017): 2107.

6. S. Mahmud, M. Rahman, M. Kamruzzaman, et al., "Recent Advances in Lithium-Ion Battery Materials for Improved Electrochemical Performance: A Review," *Results in Engineering* 15 (2022): 100472.

7. J. H. Kim, "Grand Challenges and Opportunities in Batteries and Electrochemistry," *Frontiers in Batteries and Electrochemistry* 1 (2022): 1066276.

8. R. Gonçalves, S. Lanceros-Méndez, and C. M. Costa, "Electrode Fabrication Process and Its Influence in Lithium-Ion Battery Performance: State of the Art and Future Trends," *Electrochemistry Communications* 135 (2022): 107210.

9. P. Zhu, P. R. Slater, and E. Kendrick, "Insights into Architecture, Design and Manufacture of Electrodes for Lithium-Ion Batteries," *Materials & Design* 223 (2022): 111208.

10. H. Sun, J. Zhu, D. Baumann, et al., "Hierarchical 3D Electrodes for Electrochemical Energy Storage," *Nature Reviews Materials* 4 (2018): 45–60.

11. C. Daniel, "Lithium Ion Batteries and Their Manufacturing Challenges," in *Frontiers of Engineering: Reports on Leading-Edge Engineering from the 2014 Symposium* (National Academies Press, 2015).

12. P. K. Dammala, K. B. Dermenci, A. R. Kathribail, P. Yadav, J. Van Mierlo, and M. Berecibar, "A Critical Review of Future Aspects of Digitalization Next Generation Li-Ion Batteries Manufacturing Process," *Journal of Energy Storage* 74 (2023): 109209.

13. M. N. AL-Shroofy, "*Understanding and Improving Manufacturing Processes for Making Lithium-ion Battery Electrodes*" (PhD thesis, University of Kentucky, 2018).

14. M. Schmitt, P. Scharfer, and W. Schabel, "Slot Die Coating of Lithium-Ion Battery Electrodes: Investigations on Edge Effect Issues for Stripe and Pattern Coatings," *Journal of Coatings Technology and Research* 11 (2014): 57–63.

15. I. Phiri, J.-T. Kim, S. Kennedy, M. Ravi, Y. Lee, and M.-H. Ryou, "Improvement of Electrochemical Performance of Lithium-Ion Secondary Batteries Using Double-Layered Thick Cathode Electrodes," *Journal of the Korean Electrochemical Society* 25 (2022): 32–41.

16. A. Kraytsberg and Y. Ein-Eli, "Conveying Advanced Li-Ion Battery Materials into Practice the Impact of Electrode Slurry Preparation Skills," *Advanced Energy Materials* 6 (2016): 1600655.

17. J. Li, Y. Lu, T. Yang, D. Ge, D. L. Wood, and Z. Li, "Water-Based Electrode Manufacturing and Direct Recycling of Lithium-Ion Battery Electrodes—A Green and Sustainable Manufacturing System," *iScience* 23 (2020): 101081.

18. S. C. Mun, Y. H. Jeon, and J. H. Won, "Progress and Challenges for Replacing n-Methyl-2-Pyrrolidone/Polyvinylidene Fluoride Slurry Formulations in Lithium-Ion Battery Cathodes," *Progress in Natural Science: Materials International* 34 (2024): 194–206.

19. S. N. Bryntesen, A. H. Strømman, I. Tolstorebrov, P. R. Shearing, J. J. Lamb, and O. Stokke Burheim, "Opportunities for the State-of-the-Art Production of LIB Electrodes—A Review," *Energies* 14 (2021): 1406.

20. E. Oppegård, A. Jinasena, A. Hammer Strømman, J. Are Suul, and O. Stokke Burheim, "Study of an Industrial Electrode Dryer of a Lithium-Ion Battery Manufacturing Plant: Dynamic Modeling," in *Proceedings of the 61st SIMS Conference on Simulation and Modelling SIMS 2020 (Virtual Conference)*, Vol. 176, September 22–24, 2020: 77–84.

21. N. Loeffler, J. Von Zamory, N. Laszczynski, I. Doberdo, G. T. Kim, and S. Passerini, "Performance of LiNi1/3Mn1/3Co1/3O2/Graphite Batteries Based on Aqueous Binder," *Journal of Power Sources* 248 (2014): 915–922.

22. J. Orlenius, O. Lyckfeldt, K. A. Kasvayee, and P. Johander, "Water Based Processing of LiFePO4/C Cathode Material for Li-Ion Batteries Utilizing Freeze Granulation," *Journal of Power Sources* 213 (2012): 119–127.

23. J. Shin and H. Duong, "*Electrochemical Performance of Dry Battery Electrode*," The Electrochemical Society ECS Meeting Abstracts, MA2018-01 (2018): 365.

24. J. Liu, B. Ludwig, Y. Liu, et al., "Scalable Dry Printing Manufacturing to Enable Long-Life and High Energy Lithium-Ion Batteries," *Advanced Materials Technologies* 2 (2017): 1700106.

25. B. Ludwig, Z. Zheng, W. Shou, Y. Wang, and H. Pan, "Solvent-Free Manufacturing of Electrodes for Lithium-Ion Batteries," *Scientific Reports* 6 (2016): 23150.

26. M. Al-Shroofy, Q. Zhang, J. Xu, T. Chen, A. P. Kaur, and Y. T. Cheng, "Solvent-Free Dry Powder Coating Process for Low-Cost Manufacturing of LiNi1/3Mn1/3Co1/3O2 Cathodes in Lithium-Ion Batteries," *Journal of Power Sources* 352 (2017): 187–193.

27. J. Li, C. Daniel, D. Mohanty, and D. L. Wood, "Thick Low-Cost, High-Power Lithium-Ion Electrodes via Aqueous Processing," in *DOE Annual Merit Review presentation ES164*, (U.S. Department of Energy, 2015).

28. M. D. Bouguern, A. K. Madikere Raghunatha Reddy, X. Li, S. Deng, H. Laryea, and K. Zaghib, "Engineering Dry Electrode Manufacturing for Sustainable Lithium-Ion Batteries," *Batteries* 10 (2024): 39.

29. H. M. Kim, B. Il Yoo, J. W. Yi, M. J. Choi, and J. K. Yoo, "Solvent-Free Fabrication of Thick Electrodes in Thermoplastic Binders for High Energy Density Lithium-Ion Batteries," *Nanomaterials* 12 (2022): 3320.

30. K. Uzun, B. Sharma, X. Huang, et al., "Investigating the Structure and Performance Differences between the Electrodes Made by a Dry and a Wet Slurry Processes," *The Electrochemical Society ECS Meeting Abstracts*, MA2023-01 (2023): 533.

31. W. Jin, G. Song, J. K. Yoo, S. K. Jung, T. H. Kim, and J. Kim, "Advancements in Dry Electrode Technologies: Towards Sustainable and Efficient Battery Manufacturing," *ChemElectroChem* 11 (2024): e202400288.

32. Q. Wu, J. P. Zheng, M. Hendrickson, and E. J. Plichta, "Dry Process for Fabricating Low Cost and High Performance Electrode for Energy Storage Devices," *MRS Advances* 4 (2019): 857–863.

33. M. K. Sadan and A. K. Haridas, "Solvent-Free Electrode Fabrication for Next-Generation Batteries: Inception or an Endgame?," *Chemistry–A European Journal* 31 (2025): e202501487.

34. B. Schumm, A. Dupuy, M. Lux, et al., "Dry Battery Electrode Technology: From Early Concepts to Industrial Applications," *Advanced Energy Materials* 15 (2025): 2406011.

35. J. Li, J. Fleetwood, W. B. Hawley, and W. Kays, "From Materials to Cell: State-of-the-Art and Prospective Technologies for Lithium-Ion Battery Electrode Processing," *Chemical Reviews* 122 (2021): 903–956.

36. A. Gunnarsson, E. Gunnarsson, K. Hedberg, N. Svenningsson, R. Mohammed, and Runesson, *Challenges and Opportunities with Continuous Electrode Slurry Mixing in Lithium-Ion Battery Manufacturing* (Chalmers University of Technology, 2025).

37. K. Arslan, K. B. Dermenci, J. Van Mierlo, and M. Berecibar, "Current and Future Trends in Lithium-Ion Battery Electrode Production Machinery: A Comprehensive Review," *Applied Energy* 402 (2026): 126968.

38. J. Park, J. Kim, J. Kim, M. Kim, T. Song, and U. Paik, "Sustainable and Cost-Effective Electrode Manufacturing for Advanced Lithium Batteries: The Roll-to-Roll Dry Coating Process," *Chemical Science* 16 (2025): 6598–6619.

39. H. Oh, G. S. Kim, B. U. Hwang, J. Bang, J. Kim, and K. M. Jeong, "Development of a Feasible and Scalable Manufacturing Method for PTFE-Based Solvent-Free Lithium-Ion Battery Electrodes," *Chemical Engineering Journal* 491 (2024): 151957.

40. C. D. Reynolds, H. Walker, A. Mahgoub, E. Adebayo, and E. Kendrick, "Battery Electrode Slurry Rheology and Its Impact on Manufacturing," *Energy Advances* 4 (2025): 84–93.

41. C. D. Reynolds, S. D. Hare, P. R. Slater, M. J. H. Simmons, and E. Kendrick, "Rheology and Structure of Lithium-Ion Battery Electrode Slurries," *Energy Technology* 10 (2022): 2200545.

42. P. Guichelaar, *Viscosity: The Resistance to Flow* (Tribology & Lubrication Technology, 2007).

43. E. Brown and H. M. Jaeger, "Through Thick and Thin," *Science* 333 (2011): 1230–1231.

44. E. G. Goh and W. B. Wan Nik, "A Generalized Model for Viscosity as a Function of Shear Rate," *ARPN Journal of Engineering and Applied Sciences* 13 (2018): 3219–3223.

45. P. A. Janmey and M. Schliwa, "Rheology," *Current Biology* 18 (2008): R639–R641.

46. K. Wichterle and M. Večeř, *Transport and Surface Phenomena*, (Elsevier, 2020): 89–97.

47. M. Zhang, Q. Sheng, and Z. Cui, "Time Independent Fluids," *Physics Education* 8 (1973): 333.

48. M. Singh and S. Singh, "Shear Thickening and Shear Thinning," *Survismeter: Fundamentals, Devices, and Applications*, (Jenny Standford Publishing, 2019): 305–308.

49. A. Cushing, T. Zheng, K. Higa, and G. Liu, "Viscosity Analysis of Battery Electrode Slurry," *Polymers* 13 (2021): 4033.

50. S. L. Morelly, R. M. Saraka, N. J. Alvarez, and M. Tang, "Impact of Mixing Shear on Polymer Binder Molecular Weight and Battery Electrode Reproducibility," *Batteries* 10 (2024): 46.

51. H. Nakajima, T. Kitahara, Y. Higashinaka, and Y. Nagata, "Effect of Electrode Mixing Conditions on the Performance of Lithium-Ion Batteries Analyzed by Fast Fourier Transform Electrochemical Impedance Spectroscopy," *ECS Transactions* 64 (2015): 87–95.

52. P. Galek, J. Różański, and K. Fic, "Toward Better Porous Carbon-Based Electrodes by Investigation of the Viscoelastic Properties of Carbon Suspension," *Chemical Engineering Journal* 463 (2023): 142476.

53. W. Russel, W. Russel, D. Saville, and W. Schowalter, *Colloidal Dispersions* (Cambridge University Press, 1991).

54. L. F. Pease, R. C. Daniel, and C. A. Burns, "Slurry Rheology of Hanford Sludge," *Chemical Engineering Science* 199 (2019): 628–634.

55. A. Knight, F. Sofrà, A. Stickland, P. Scales, D. Lester, and R. Buscall, "Variability of Shear Yield Stress – Measurement and Implications for Mineral Processing," A. Wu & R. Jewell (eds), in *Proceedings of the 20th International Seminar on Paste and Thickened Tailings*, (University of Science and Technology Beijing, 2017): 57–65.

56. W. B. Hawley and J. Li, "Beneficial Rheological Properties of Lithium-Ion Battery Cathode Slurries from Elevated Mixing and Coating Temperatures," *Journal of Energy Storage* 26 (2019): 100994.

57. L. Ouyang, Z. Wu, J. Wang, et al., "The Effect of Solid Content on the Rheological Properties and Microstructures of a Li-Ion Battery Cathode Slurry," *RSC Advances* 10 (2020): 19360–19370.

58. R. G. Morgan, S. K. S. Pindiprolu, B. Balaraman, G. S. Pangu, "*Combined Rheometer/Mixer Having Helical Blades and Methods of Determining Rheological Properties of Fluid*s," US20140311225A1 (Halliburton Energy Services Inc, 2017).

59. J. V. Koleske, *Paint and Coating Testing Manual : Fourteenth Edition of the Gardner-Sward Handbook* (ASTM, 1995).

60. G. Alsofi, C. Reynolds, and E. Kendrick, Optimization of Hard Carbon Anodes in Sodium-Ion Batteries [Online Poster], BatteryDesign.Net From Chemistry To Pack, 2022.

61. C. Reynolds, M. Faraji Niri, M. F. Hidalgo, et al., "Impact of Formulation and Slurry Properties on Lithium-Ion Electrode Manufacturing," *Batteries & Supercaps* 7 (2024): e202300396.

62. J. Li, C. Rulison, J. Kiggans, C. Daniel, and D. L. Wood, "Superior Performance of LiFePO. 4 Aqueous Dispersions via Corona Treatment and Surface Energy Optimization," *Journal of the Electrochemical Society* 159 (2012): A1152–A1157.

63. F. Ghani, K. An, D. A. Lee, F. Ghani, K. An, and D. Lee, "A Review on Design Parameters for the Full-Cell Lithium-Ion Batteries," *Batteries* 10 (2024): 340.

64. H. Nakamura, T. Kawaguchi, T. Masuyama, et al., "Dry Coating of Active Material Particles with Sulfide Solid Electrolytes for an All-Solid-State Lithium Battery," *Journal of Power Sources* 448 (2020): 227579.

65. J. Liu, B. Ludwig, Y. Liu, H. Pan, and Y. Wang, "Strengthening the Electrodes for Li-Ion Batteries with a Porous Adhesive Interlayer through Dry-Spraying Manufacturing," *ACS Applied Materials & Interfaces* 11 (2019): 25081–25089.

66. R. Tao, B. Steinhoff, C. H. Sawicki, et al., "Unraveling the Impact of the Degree of Dry Mixing on Dry-Processed Lithium-Ion Battery Electrodes," *Journal of Power Sources* 580 (2023): 233379.

67. A. Gyulai, W. Bauer, and H. Ehrenberg, "Dry Electrode Manufacturing in a Calender: The Role of Powder Premixing for Electrode Quality and Electrochemical Performance," *ACS Applied Energy Materials* 6 (2023): 5122–5134.

68. N. M. Nurazzi, M. R. M. Asyraf, M. Rayung, et al., "Thermogravimetric Analysis Properties of Cellulosic Natural Fiber

Polymer Composites: A Review on Influence of Chemical Treatments," *Polymers* 13 (2021): 2710.

69. L. A. Gomez-Moreno, A. Klemettinen, and R. Serna-Guerrero, "A Simple Methodology for the Quantification of Graphite in End-of-Life Lithium-Ion Batteries Using Thermogravimetric Analysis," *iScience* 26 (2023): 107782.

70. M. E. Sotomayor, C. de la Torre-Gamarra, B. Levenfeld, et al., "Ultra-Thick Battery Electrodes for High Gravimetric and Volumetric Energy Density Li-Ion Batteries," *Journal of Power Sources* 437 (2019): 226923.

71. A. Maurel, R. Russo, S. Grugeon, S. Panier, and L. Dupont, "Environmentally Friendly Lithium-Terephthalate/Polylactic Acid Composite Filament Formulation for Lithium-Ion Battery 3D-Printing via Fused Deposition Modeling," *ECS Journal of Solid State Science and Technology* 10 (2021): 037004.

72. Z. Zhang, D. Han, M. Xiao, et al., "New Potential Substitute of PVDF Binder: Poly(propylene Carbonate) for Solvent-Free Manufacturing High-Loading Cathodes of LiFePO4|Li Batteries," *Ionics* 29 (2023): 3895–3906.

73. G. A. B. Matthews, S. Wheeler, J. Ramírez-González, and P. S. Grant, "Solvent-Free NMC Electrodes for Li-Ion Batteries: Unravelling the Microstructure and Formation of the PTFE Nano-Fibril Network," *Frontiers in Energy Research* 11 (2023): 1336344.

74. R. Tao, Y. Gu, Z. Du, X. Lyu, and J. Li, "Advanced Electrode Processing for Lithium-Ion Battery Manufacturing," *Nature Reviews Clean Technology* 1, no. 2 (2025): 116–131.

75. B. E. El Mohajir and N. Heymans, "Changes in Structural and Mechanical Behaviour of PVDF with Processing and Thermomechanical Treatments. 1. Change in Structure," *Polymer* 42 (2001): 5661–5667.

76. H. Duong, A. Suszko, and H. Feigenbaum, "(Invited) Dry Electrode Process Technology,"*The Electrochemical Society ECS Meeting Abstracts*, MA2016-01 (2016): 475.

77. D. Schulze, J. Schwedes, and J. W. Carson, "*Powders and Bulk Solids: Behavior, Characterization, Storage and Flow*," (Springer, 2008): 1–511.

78. Z. Cheng, J. H. Leal, C. E. Hartford, et al., "Flow Behavior Characterization of Biomass Feedstocks," *Powder Technology* 387 (2021): 156–180.

79. M. Medhe, B. Pitchumani, and J. Tomas, "Flow Characterization of Fine Powders Using Material Characteristic Parameters," *Advanced Powder Technology* 16 (2005): 123–135.

80. B. Düsenberg, J. Schmidt, I. Sensoy, and A. Bück, "Flowability of Plant Based Food Powders: Almond, Chestnut, Chickpea, Coconut, Hazelnut and Rice," *Journal of Food Engineering* 357 (2023): 111606.

81. C. Lischka, S. Gerl, J. Kappes, A. Chauhan, and H. Nirschl, "Experimental & Simulative Assessment of Mixing Quality for Dry Li-Ion Cathode Production in an Eirich Intensive Mixer," *Powder Technology* 431 (2024): 119072.

82. S. Tschöcke, H. Althues, B. Schumm, et al., "*Process for Producing a Dry Film and Dry Film and Dry Film Coated Substrate*," DE102017208220A1 (Technische Universitaet Dresden and Fraunhofer Gesellschaft Zur Foerderung der Angewandten Forschung eV, 2017).

83. K. J. Bigham, "*Drawn Fiber Polymers: Chemical and Mechanical Features*," (Zeus Ind. Prod. Ltd, 2018): 1–32.

84. C. J. Drummond, G. Georgaklis, and D. Y. C. Chan, "Fluorocarbons: Surface Free Energies and Van der Waals Interaction," *Langmuir* 12 (1996): 2617–2621.

85. B. Zou, L. Zhong, P. Mitchell, X. Xi, "*Dry-Particle Packaging Systems and Methods of Making Same*," US20060137158A1 (Maxwell Technologies Inc, 2006).

86. P. Mitchell, L. Zhong, X. Xi, "*Recyclable Dry Particle Based Adhesive Electrode and Methods of Making Same*," US7342770B2 (Maxwell Technologies Inc, 2008).

87. P. Mitchell, L. Zhong, X. Xi, and B. Zou, "*Dry-Particle Based Adhesive and Dry Film and Methods of Making Same*," US7508651B2 (Maxwell Technologies Inc, 2009).

88. F. Hippauf, B. Schumm, S. Doerfler, et al., "Overcoming Binder Limitations of Sheet-Type Solid-State Cathodes Using a Solvent-Free Dry-Film Approach," *Energy Storage Materials* 21 (2019): 390–398.

89. L. Zhong, "*Electrode for Energy Storage Devices and Method of Making Same*," US10069131B2 (LICAP Technologies Inc, 2018).

90. L. Zhong, S. Erika, B. K. Kim, "*Dry Electrode Manufacture with Lubricated Active Material Mixture*," US20230056854A1 (LiCAP Technologies Inc, 2022).

91. A. Korolev, M. Mishnev, D. Zherebtsov, N. I. Vatin, and M. Karelina, "Polymers under Load and Heating Deformability: Modelling and Predicting," *Polymers* 13 (2021): 428.

92. A. Abdelbary, "Sliding Mechanics of Polymers," In *Wear of Polymers and Composites*, (Woodhead Publishing, 2014): 37–66.

93. K. Qiu, E. Shaw, M. Zea, L. Zhong, "*Dry Electrode Manufacture by Temperature Activation Method*," US-20200388822-A1 (Licap Technologies Inc, 2020).

94. C. Johnson, "How the Safe Drinking Water Act & the Comprehensive Environmental Response, Compensation, and Liability Act Fail Emerging Contaminants: A Per- and Polyfluoroalkyl Substances (PFAS) Cast Study," *Mitchell Hamline Law Journal of Public Policy and Practice* 42 (2021): 91–137.

95. J. Black, A. Moreland, M. M. Ransom, and E. Sanchez, "Perfluoroalkyl and Polyfluoroalkyl Substances: Using Law and Policy to Address These Environmental Health Hazards in the United States," *Health Matrix: Journal of Law-Medicine* 31 (2021): 341.

96. N. M. Brennan, A. T. Evans, M. K. Fritz, S. A. Peak, and H. E. von Holst, "Trends in the Regulation of Per-and Polyfluoroalkyl Substances (PFAS): A Scoping Review," *International Journal of Environmental Research and Public Health* 18 (2021): 10900.

97. H. M. Doung, H. Feigenbaum, J. Hong, "*Dry Energy Storage Device Electrode and Methods of Making the Same*," US010741843B2 (Maxwell Technologies Inc, 2015).

98. J. Kang, H. Eom, S. Jang, et al., "Bollard-Anchored Binder System for High-Loading Cathodes Fabricated via Dry Electrode Process for Li-Ion Batteries," *Advanced Materials* 37 (2025): 2416872.

99. K. E. Sung, I. Hwang, J. Choi, S. K. Jung, and J. Yoon, "Enhanced Adhesion in PTFE-Based Dry Electrodes with Hydrogen Bonding Co-Binder Integration for Advanced Lithium-Ion Batteries," *Chemical Engineering Journal* 511 (2025): 161789.

100. D. L. Wood, J. D. Quass, J. Li, S. Ahmed, D. Ventola, and C. Daniel, "Technical and Economic Analysis of Solvent-Based Lithium-Ion Electrode Drying with Water and NMP," *Drying Technology* 36 (2018): 234–244.

101. D. L. Wood, M. Wood, J. Li, et al., "Perspectives on the Relationship between Materials Chemistry and Roll-to-Roll Electrode Manufacturing for High-Energy Lithium-Ion Batteries," *Energy Storage Materials* 29 (2020): 254–265.

102. C. D. Reynolds, P. R. Slater, S. D. Hare, M. J. H. Simmons, and E. Kendrick, "A Review of Metrology in Lithium-Ion Electrode Coating Processes," *Materials & Design* 209 (2021): 109971.

103. L. A. Román-Ramírez, G. Apachitei, M. Faraji-Niri, M. Lain, D. Widanage, and J. Marco, "Effect of Coating Operating Parameters on Electrode Physical Characteristics and Final Electrochemical Performance of Lithium-Ion Batteries," *International Journal of Energy and Environmental Engineering* 13 (2022): 943–953.

104. L. A. Román-Ramírez, G. Apachitei, M. Faraji-Niri, M. Lain, W. D. Widanage, and J. Marco, "Understanding the Effect of Coating-Drying Operating Variables on Electrode Physical and Electrochemical

Properties of Lithium-Ion Batteries," *Journal of Power Sources* 516 (2021): 230689.

105. M. Faraji Niri, C. Reynolds, L. A. Román Ramírez, E. Kendrick, and J. Marco, "Systematic Analysis of the Impact of Slurry Coating on Manufacture of Li-Ion Battery Electrodes via Explainable Machine Learning," *Energy Storage Materials* 51 (2022): 223–238.

106. E. Kendrick, in *Future Lithium-Ion Batteries*, ed. A. Eftekhari (Royal Society Of Chemistry, 2019): 262–289.

107. A. Etiemble, N. Besnard, J. Adrien, et al., "Quality Control Tool of Electrode Coating for Lithium-Ion Batteries Based on X-Ray Radiography," *Journal of Power Sources* 298 (2015): 285–291.

108. A. du Baret de Limé, T. Lein, S. Maletti, et al., "Impact of Electrode Defects on Battery Cell Performance: A Review," *Batteries & Supercaps* 5 (2022): e202200239.

109. A. Schoo, R. Moschner, J. Hülsmann, and A. Kwade, "Coating Defects of Lithium-Ion Battery Electrodes and Their Inline Detection and Tracking," *Batteries* 9 (2023): 111.

110. Y. S. Zhang, N. E. Courtier, Z. Zhang, et al., "A Review of Lithium-Ion Battery Electrode Drying: Mechanisms and Metrology," *Advanced Energy Materials* 12 (2022): 2102233.

111. M. Nikpour, B. Liu, D. Wheeler, and B. A. Mazzeo, "Li-Ion Electrode Microstructure Evolution during Drying and Calendering," *The Electrochemical Society ECS Meeting Abstracts*, MA2021-02 (2021): 438.

112. H. Hagiwara, W. J. Suszynski, and L. F. Francis, "A Raman Spectroscopic Method to Find Binder Distribution in Electrodes during Drying," *Journal of Coatings Technology and Research* 11 (2014): 11–17.

113. S. Jaiser, M. Müller, M. Baunach, W. Bauer, P. Scharfer, and W. Schabel, "Investigation of Film Solidification and Binder Migration during Drying of Li-Ion Battery Anodes," *Journal of Power Sources* 318 (2016): 210–219.

114. E. R. Ezeigwe, R. N. Dunne, S. B. B. Solberg, J. J. Lamb, J. Wind, and O. S. Burheim, "Manufacturing Techniques for Improved Rate Capacity of Thick Electrodes by Tailored Electrode Structures," *Journal of Energy Storage* 109 (2025): 115253.

115. M. Prasad, S. Hein, T. Danner, and A. Latz, "Effect of a Heterogeneous Distribution of the Conductive Additives and Binder Domain on the Impedances of Lithium-Ion Battery Electrodes," *The Electrochemical Society ECS Meeting Abstracts*, MA2022-01 (2022): 266.

116. C. Busà, M. Belekoukia, and M. J. Loveridge, "The Effects of Ambient Storage Conditions on the Structural and Electrochemical Properties of NMC-811 Cathodes for Li-Ion Batteries," *Electrochimica Acta* 366 (2021): 137358.

117. S. Wolf, L. Garbade, V. Göken, et al., "Process and Material Analysis of Laser- and Convection-Dried Silicon–Graphite Anodes for Lithium-Ion Batteries," *World Electric Vehicle Journal* 14 (2023): 87.

118. M. W. von Horstig, A. Schoo, T. Loellhoeffel, J. K. Mayer, and A. Kwade, "A Perspective on Innovative Drying Methods for Energy-Efficient Solvent-Based Production of Lithium-Ion Battery Electrodes," *Energy Technology* 10 (2022): 2200689.

119. M. Abdollahifar, H. Cavers, S. Scheffler, A. Diener, M. Lippke, and A. Kwade, "Insights into Influencing Electrode Calendering on the Battery Performance," *Advanced Energy Materials* 13 (2023): 2300973.

120. D. Wang, G. Wang, C. Xu, and H. Liu, "Mechanics and Deformation Behavior of Lithium-Ion Battery Electrode during Calendering Process," *Journal of Energy Storage* 87 (2024): 111521.

121. X. Lu, S. R. Daemi, A. Bertei, et al., "Microstructural Evolution of Battery Electrodes During Calendering," *Joule* 4 (2020): 2746–2768.

122. C. Meyer, H. Bockholt, W. Haselrieder, and A. Kwade, "Characterization of the Calendering Process for Compaction of Electrodes for Lithium-Ion Batteries," *Journal of Materials Processing Technology* 249 (2017): 172–178.

123. W. Haselrieder, S. Ivanov, D. K. Christen, H. Bockholt, and A. Kwade, "Impact of the Calendering Process on the Interfacial Structure and the Related Electrochemical Performance of Secondary Lithium-Ion Batteries," *ECS Transactions* 50 (2013): 59–70.

124. K. Huber, S. Stojcevic, M. Wolf, and A. Kwade, "Dry Battery Electrode Manufacturing Enabled By Continuous Powder Mixing," *The Electrochemical Society ECS Meeting Abstracts*, MA2023-01 (2023): 539.